NATIONAL ADVISORY COMMITTEE FOR AERONAUTICS

TECHNICAL NOTE

No. 1338

PROPELLER-EFFICIENCY CHARTS FOR LIGHT AIRPLANES

By John L. Crigler and Robert E. Jaquis

Langley Memorial Aeronautical Laboratory
Langley Field, Va.

Washington
July 1947

NATIONAL ADVISORY COMMITTEE FOR AERONAUTICS

TECHNICAL NOTE NO. 1338

PROPELLER-EFFICIENCY CHARTS FOR LIGHT AIRPLANES

By John L. Crigler and Robert E. Jaquis

SUMMARY

The selection of a propeller on the basis of efficiency for application to a light-airplane design can be accomplished by the use of the charts presented. The required calculations are made a minimum by presenting the dimensional propeller parameters directly on the charts. Values of power of 50, 100, 150, 225, and 300 horsepower are covered for airspeeds of 50, 100, 150, and 200 miles per hour, propeller diameters of 6, 8, and 10 feet, and blade numbers of two, four, six, and eight over a wide range of propeller rotational speed.

The application of the results to design problems is demonstrated by three examples: (1) the investigation of the efficiency of a wide variety of propellers for a given design condition, (2) the investigation of the efficiency of a controllable-pitch constant-speed propeller as a function of airspeed, and (3) the investigation of the efficiency of a fixed-pitch propeller as a function of airspeed and engine operation.

INTRODUCTION

The operation of light airplanes near residential neighborhoods presents the problem of noise reduction. One of the sources of airplane noise is the airplane propeller. In many instances the noise can be reduced by the proper selection of the airplane propeller. The problem of the efficiency of the quiet propeller, however, is also of importance. The present paper gives the efficiency of a wide selection of airplane propellers for light airplanes to aid in the required compromise between efficiency and noise reduction or any other operational or design condition.

Selection charts for propellers are presented in reference 1. The range of low advance-diameter ratio, however, is not covered in these charts. The present paper gives charts for values of advance-diameter ratio down to 0.314. The calculated efficiency for propellers of optimum load distribution along the blade for

a given operating condition is presented. The advantage of using this efficiency is that it presents a maximum value that cannot be exceeded with a given propeller diameter and blade number but can be obtained with proper design. The methods of analysis are given in the appendix. Comparisons of the calculated efficiencies with experimental data on propellers show good agreement.

The selection charts given herein present directly the efficiencies as a function of the propeller operating conditions. Investigation of a given propeller for application to a given design condition requires nothing more than the reading of a few charts and interpolating between these charts to obtain the results.

SYMBOLS

a	axial-velocity interference factor
B	number of propeller blades
b	chord of propeller blade element
c_d	section drag coefficient (d/qA)
c_l	section lift coefficient (L/qA)
C_P	power coefficient $(P/\rho n^3 D^5)$
C_Q	torque coefficient $(Q/\rho n^2 D^5)$
C_T	thrust coefficient $(T/\rho n^2 D^4)$
D	propeller diameter
d	drag of propeller blade element for infinite aspect ratio
J	advance-diameter ratio (V/nD)
l	lift of blade section
N	propeller rotational speed, revolutions per minute
n	propeller rotational speed, revolutions per second
P	input power to propeller
P_c	power disk-loading coefficient (P/qAV)

$$\frac{1}{\sqrt{P_c}} = D\sqrt{\frac{\pi\rho V^3}{8P}}$$

Q	torque of propeller
q	dynamic pressure of air stream
R	tip radius
r	radius to any blade element
A	disk area of propeller
T	thrust of propeller
V	axial velocity of propeller
x	radial location of blade element (r/R)
$\frac{dC_Q}{dx}$	element torque coefficient $\left(\frac{dQ/dx}{\rho n^2 D^5}\right)$
$\frac{dC_T}{dx}$	element thrust coefficient $\left(\frac{dT/dx}{\rho n^2 D^4}\right)$
η	propeller efficiency
η_i	ideal propeller efficiency $\left(\frac{1}{1+a}\right)$; $P_c = \frac{4(1-\eta_i)}{\eta_i^3}$
$\eta_{opt.}$	efficiency with optimum load distribution without drag
ρ	mass density of air
σ	propeller-element solidity $\left(\frac{Bb}{2\pi r}\right)$
σc_l	propeller-element load coefficient
ϕ	angle of inclination of resultant velocity to plane of rotation

Subscripts:

0.7R	at 0.7 radius
D	due to drag

RESULTS

Propeller efficiencies for light airplanes are presented in terms of engine power, velocity, blade number, blade diameter, and propeller rotational speed for the use of light-airplane manufacturers and operators. A wide range of propeller selection is presented in order to permit evaluation of the efficiencies obtained with high-solidity low-rotational-speed propellers compared with low-solidity high-rotational-speed propellers. The charts are intended to cover the requirements that may be needed in the study of the sound reduction of light-airplane propellers. The scope of the results and a key to figures 1 to 22 are given in table I.

Figure 1 shows the breakdown of the propeller losses for one condition and will aid in interpreting the results presented in the other figures. The value of the ideal efficiency η_i given for figure 1 is the value obtained from consideration of the minimum momentum increase in the wake. Only axial momentum and a uniform increase in velocity over the entire disk area are considered. The ideal efficiency is given by the relationship $P_c = \frac{4(1 - \eta_i)}{\eta_i^3}$ and is fixed for a given power, velocity, and propeller diameter. The shaded area in the figure shows the induced losses for propellers having optimum efficiency. The optimum efficiency η_{opt} is the efficiency (without drag) for a propeller with an optimum load distribution as given by Goldstein for the specified number of blades. This efficiency considers the rotational and axial momentum of the wake and distributes the loading along the blade so that the integrated sum of the losses is a minimum.

The propeller efficiency η given in all the figures is obtained by subtracting the blade drag from the optimum efficiency. The magnitude of the blade drag can be seen to vary greatly with the section loading. In figure 1 the low-solidity propeller is highly loaded at low rotational speed and is very close to the stall condition at 1250 rpm. The approach to stall is indicated when the propeller efficiency η and the optimum efficiency η_{opt} begin to diverge. At high rotational speed the blade sections for the low-solidity propeller are operating at or near maximum lift-drag ratio and, therefore, show the highest efficiency. The high-solidity propeller is operating at very light loading (low value of c_l for the section) and, therefore, at a very low lift-drag ratio. At 2000 rpm the blade drag loss has increased from 8 percent for the low-solidity propeller to 32 percent for the high-solidity propeller.

The values of ideal efficiency, optimum efficiency, and resultant propeller efficiency are given in each of figures 1 to 22 in order to permit insight into the losses sustained for each operating condition.

Figures 1 to 3 give efficiency as a function of propeller rotational speed for 6-, 8-, and 10-foot-diameter four-blade propellers of varying solidities ($\sigma = 0.069$ to $\sigma = 0.276$) for engine power of 300 horsepower for two forward speeds. The difference between the calculated propeller efficiencies (drag included) for each solidity and the optimum efficiency is due to blade drag. The drag varies rapidly with propeller solidity and propeller rotational speed. In all the present calculations the propeller rotational speed is limited so that the value of πnD does not exceed 950 feet per second (Mach number, 0.85). Although small compressibility losses may result at this Mach number, no losses were included in the calculations.

In figures 4 to 22 the calculated efficiency is plotted against propeller rotational speed for velocities of 50, 100, 150, and 200 miles per hour at engine powers of 50, 100, 150, 225, and 300 horsepower. In each case the propeller solidity is 0.0345B and, therefore, the total solidity increases proportionally to the blade number. The efficiencies for other total solidities and blade numbers can be obtained from the charts by the use of figure 5. For optimum propellers with geometrically similar blade sections, the principal change in efficiency resulting from changing the blade number and holding the solidity constant is due to a change in the optimum efficiency. In figure 5 the optimum efficiency is shown for two-, four-, and eight-blade propellers. The number of blades is seen to affect the optimum efficiency - the greater the number of blades the higher the efficiency. The magnitude of this change in η_{opt} with blade number, however, is seen to be small and close estimates of the efficiencies to be realized for constant-solidity propellers with a change in blade number can be made. The drag losses may vary for constant solidity and different blade numbers because of changes in the airfoil characteristics with Reynolds number but, in general, this effect is very small and is not considered in the present paper.

EXAMPLES

I - Propeller Selection for One Design Condition

The charts of the present paper show the efficiencies of a large number of propellers that could be fitted to a given design condition. Example I is given to explain the use of the charts.

The design conditions for a given airplane are as follows: The 150-horsepower engine operates at 2700 rpm. The design velocity is 150 miles per hour. The propeller rotational speed with direct and gear drives can be chosen as 2700, 1800, 1350, or 900 rpm.

The following table gives values of efficiency for some of the propellers that could be fitted to the given airplane. All the propellers for this set of design conditions are taken from figure 14.

N (rpm)	D	B	η	N (rpm)	D	B	η
2700	6	2	83.5	1350	8	6	79.0
2700	6	4	71.0	1350	8	8	71.5
1800	6	2	83.5	1350	10	2	85.0
1800	6	4	84.0	1350	10	4	68.0
1800	6	6	81.0	900	6	6	72.0
1800	6	8	73.5	900	6	8	73.5
1800	8	2	87.0	900	8	4	85.0
1800	8	4	77.5	900	8	6	83.5
1350	6	4	81.0	900	8	8	81.0
1350	6	6	81.0	900	10	2	87.0
1350	6	8	77.0	900	10	4	83.0
1350	8	2	86.5	900	10	6	76.5
1350	8	4	84.5	900	10	8	71.5

Many of these propellers are close to stalling at 150 miles per hour and at lower velocity would stall and give very poor efficiency. Investigation of any propeller for a range of velocities is taken up in example II for a controllable-pitch constant-speed propeller and in example III for the fixed-pitch propellers.

II - Controllable-Pitch Constant-Speed Propeller

Figure 23 is a cross plot of the propeller efficiency as a function of the forward velocity for a 100-horsepower engine operating at constant speed. The curves in figure 23(a) show the efficiencies for an 8-foot-diameter two-blade propeller and the curves in figure 23(b) show the efficiencies for a 6-foot-diameter six-blade propeller. The data for these curves were obtained from figures 16 to 19 and are very close approximations to the efficiencies that would be obtained for controllable-pitch constant-speed propellers of the same diameter and solidity. In a similar manner the propeller efficiency for constant rotational speed can be obtained from the

figures for any combination of engine power, propeller diameter, blade number, and range of forward velocity covered in the study.

III - Propeller Performance for Fixed-Pitch Operation

In order to determine the variation of the performance with airspeed of a given propeller for fixed-pitch operation, it is necessary to determine the variation of the engine speed and brake horsepower with airspeed. Since an engine operates at approximately constant torque the variation of engine speed with velocity depends on the propeller characteristics. An example is given to illustrate the procedure.

Consider a 6-foot-diameter four-blade $\left(\sigma_{0.7R} = 0.138\right)$ fixed-pitch propeller designed to absorb 150 horsepower at 1800 rpm at 150 miles per hour. Calculate C_p as follows:

$$C_p = \frac{P}{\rho n^3 D^5}$$

$$= \frac{2\pi Q}{\rho D^5 n^2}$$

$$= \frac{150 \times 550}{0.002378 \left(\frac{1800}{60}\right)^3 (6)^5}$$

$$= 0.1655$$

The value $\frac{2\pi Q}{\rho D^5}$ remains constant over the speed range. Therefore

$$n^2 C_p = 0.1655 \left(\frac{1800}{60}\right)^2$$

$$= 149$$

For the design condition

$$\frac{V}{nD} = 150 \frac{88}{60} \frac{60}{1800} \frac{1}{6}$$

$$= 1.221$$

Use experimental or calculated data for the selected propeller, if available, or use a set of curves of C_p against V/nD at various values of pitch setting for some value of $\sigma_{0.7R}$ of about 0.138. The number of blades for the test results is not very important since only the shape of the curve is required. Plot V/nD against C_p on a transparent sheet of paper and place it over the curves of experimental data. Through the given point fair in a representative curve for the variation of C_p with V/nD for the fixed pitch in question as is done in figure 24. This curve will approximate the variation of the design propeller as closely as is possible without specific experimental tests of the propeller.

In order to calculate the performance at 100 miles per hour, assume a value of V/nD a little higher than the ratio of airspeeds would give since the rotational propeller speed is going to be reduced. Thus the calculated value is given by

$$\frac{V}{nD} = 1.221 \frac{100}{150}$$

$$= 0.814$$

Try, as a first approximation, $\frac{V}{nD} = 0.85$. Then

$$n = \frac{V}{D} \frac{nD}{V}$$

$$= \frac{100 \times 1.467}{6 \times 0.85}$$

$$= 28.75$$

and

$$C_P = \frac{149}{(28.75)^2}$$

$$= 0.180$$

Plot the point $C_P = 0.180$, $\frac{V}{nD} = 0.85$ on the curve. It is seen that this point falls below the curve and that a higher value of V/nD is required. Try $\frac{V}{nD} = 0.95$. Then

$$n = \frac{146.7}{6 \times 0.95}$$

$$= 25.70$$

and

$$C_P = \frac{149}{(25.7)^2}$$

$$= 0.225$$

Since the point $C_P = 0.225$, $\frac{V}{nD} = 0.95$ falls on the curve, the value of V/nD is correct, and

$$N = (25.70)(60)$$

$$= 1540 \text{ rpm}$$

The brake horsepower is reduced by the ratio of $\frac{1540}{1800}$ or reduced from 150 to 128 horsepower.

The efficiencies for 150 miles per hour and 150 horsepower are read from figure 14 at 1800 rpm as $\eta_{opt} = 90$ percent, $\eta = 84$ percent, and $\Delta\eta_D = 6$ percent. It is necessary to read the curves for 100 miles per hour at 100 and 150 horsepower for 1540 rpm and to estimate the

efficiency at 128 horsepower. The efficiencies for 100 miles per hour and 100 horsepower are read from figure 17 at 1540 rpm as η_{opt} = 84.5 percent, η = 80 percent, and $\Delta\eta_D$ = 4.5 percent. The efficiencies for 100 miles per hour and 150 horsepower are read from figure 13 at 1540 rpm as η_{opt} = 80 percent, η = 76.5 percent, and $\Delta\eta_D$ = 3.5 percent. It should be noted that the propeller efficiency for the condition of 150 horsepower at 1540 rpm is close to the stall region. This stalling condition will require some care in estimating the efficiency by this method if the propeller is stalled at the higher engine power. An accurate determination of the propeller efficiency near the propeller stalling condition cannot be made without specific experimental data on the propeller and airplane combination. The efficiency for 128 horsepower at 100 miles per hour falls between the value of 76.5 percent for 150 horsepower and the value of 80 percent for 100 horsepower, probably at about 78.5 percent. Then

$$\text{Thrust horsepower} = 128 \times 0.785$$

$$= 100.5$$

The procedure for other velocities is a repetition of the foregoing calculation.

A breakdown of the power losses as shown gives a good indication of the possibility of obtaining a gain in efficiency by increasing the propeller solidity. If $\Delta\eta_D$ is small there is not much to be gained by increasing the solidity.

APPLICATION TO SPECIFIC DESIGN

The charts presented herein permit the selection of the primary propeller parameters - namely, diameter, rotational speed, blade number, and solidity - required for a given design condition. A comparison of the efficiencies for a wide variety of these parameters shows large changes in efficiency. The large change in efficiency demonstrates the importance of a careful selection of the primary propeller parameters. Whenever any of the primary propeller parameters are affected by considerations of noise output, ground clearance, and so forth, the present paper is particularly useful in determining the best compromise.

The secondary parameters such as pitch distribution, plan form, thickness distribution, and airfoil section are not directly treated herein. An estimate of their effect can be obtained, however, by the use of the charts. The optimum load distribution means that the product of the chord and the lift coefficient (bc_l) is a definite value for each radius at a given design condition. Small departures from the optimum load distribution do not cause appreciable changes in the efficiency. Either the pitch distribution or the plan form can be altered to obtain the optimum load distribution. Which alteration is made to give this loading is unimportant. When results of tests of pitch distribution or blade plan form show large losses in efficiency, they are caused by the changes in the drag loss due to stalling of some of the sections or to operating of some of the sections at very low lift coefficient at which the drag is large in comparison with the lift.

Blade section and thickness distribution affect the blade drag loss of the propeller. If this blade drag loss $(\Delta\eta_D$ from the charts) is small, only small effects can be expected. For operation at section lift coefficients in the range of c_l from 0.3 to 0.7 this drag loss is small for normal airfoil sections operating below critical Mach numbers. If the element lift coefficients are outside this range, the drag losses become important.

Once the primary parameters are selected the next step is the physical design of the propeller, which consists of designing the pitch distribution and blade-chord distribution to obtain the proper distribution of loading along the radius. One method of designing a propeller to give the optimum distribution of loading for any operating condition is outlined in reference 2.

Langley Memorial Aeronautical Laboratory
National Advisory Committee for Aeronautics
Langley Field, Va., July 2, 1947

APPENDIX

CONSTRUCTION OF CHARTS, METHODS AND ASSUMPTIONS

The propeller-performance curves given herein were obtained for most of the range by the method given in reference 1. In reference 1 charts are presented giving the maximum possible propeller efficiencies without drag for a wide range of operating condition. The charts were prepared for the optimum distribution of loading along the blade as given by Goldstein for light loadings. The effect of drag was added to the induced loss to obtain the propeller efficiencies given herein. Comparison of experimental data on propellers in current use with data obtained by the present method of analysis shows good agreement over the normal range of operation. For light blade loadings $\left(c_{l_{0.7R}} \text{ below } 0.15\right)$ and heavy blade loadings $\left(c_{l_{0.7R}} \text{ above } 0.8\right)$, element calculations by the methods given in reference 3 were used.

In the present paper, performance charts similar to those in reference 1 are given for values of V/nD down to 0.314 $(\pi/10)$. These charts are presented in figure 25 for two-, four-, six-, and eight-blade propellers. The ordinates give values of the optimum efficiency for propellers without drag and the abscissas represent values of $\frac{1}{\sqrt{P_c}} = D\sqrt{\frac{\pi\rho V^3}{8P}}$. Against these scales, curves of constant element load coefficient $\left(\sigma c_l\right)_{0.7R}$ are crossed by curves of constant V/nD. These charts, thus, not only give the optimum propeller efficiency with drag neglected but, with operating V/nD and $\frac{1}{\sqrt{P_c}} = D\sqrt{\frac{\pi\rho V^3}{8P}}$ known, give the required blade loading (solidity times the lift coefficient at the 0.7 radius).

The effect of blade profile drag on the propeller efficiency is also given in charts. The following formulas, taken from reference 1, give the effect of drag on the thrust and torque coefficients for zero loading:

$$\frac{dC_T}{dx} = -\sigma c_d \frac{\pi x}{4} J\sqrt{J^2 + (\pi x)^2} \qquad (1)$$

and

$$\frac{dC_Q}{dx} = \sigma c_d \frac{\pi^2 x^3}{8} \sqrt{J^2 + (\pi x)^2} \tag{2}$$

These formulas, modified to include induced velocities and to apply for any loading, are

$$\frac{dC_T}{dx} = \sigma c_d \frac{\pi x}{4} \frac{J^2(1 + a)^2}{\sin \phi} \tag{3}$$

and

$$\frac{dC_Q}{dx} = \sigma c_d \frac{\pi x^2}{8} \frac{J^2(1 + a)^2}{\sin^2 \phi} \cos \phi \tag{4}$$

The results of the integrated thrust and the integrated power coefficients due to drag calculated by the zero-loading formulas and the formulas including the induced velocities were compared for several blade loadings and each blade number. The results for the four-blade propeller with $(\sigma c_l)_{0.7R} = 0.09$ and optimum load distribution along the blade are shown in figure 26. The difference in the thrust and power coefficients due to drag and the resultant efficiency computed by the two sets of formulas were small and therefore the drag losses were computed for only one loading for each blade number and these coefficients were applied to all values of $(\sigma c_l)_{0.7R}$. The values of $(\sigma c_l)_{0.7R}$ for which drag losses were computed were $(\sigma c_l)_{0.7R} = 0.04$ for the two-blade propellers, $(\sigma c_l)_{0.7R} = 0.09$ for the four-blade propellers, $(\sigma c_l)_{0.7R} = 0.14$ for the six-blade propellers, and $(\sigma c_l)_{0.7R} = 0.18$ for the eight-blade propellers.

The distribution of c_d along the blade was determined by use of the thickness distribution and plan form of a conventional propeller operating at the blade loading for optimum distribution. The distribution of c_d used was the same as that on the propeller of reference 1. The change in profile-drag coefficients is very small for a wide range of lift coefficient so that average values were used in the calculations. Because the profile drag increases rapidly near the stalling angle, it was necessary to make element calculations to obtain the propeller performance for heavily loaded blades.

REFERENCES

1. Crigler, John L., and Talkin, Herbert W.: Charts for Determining Propeller Efficiency. NACA ACR No. L4I29, 1944.

2. Crigler, John L., and Talkin, Herbert W.: Propeller Selection from Aerodynamic Considerations. NACA ACR, July 1942.

3. Crigler, John L.: Comparison of Calculated and Experimental Propeller Characteristics for Four-, Six-, and Eight-Blade Single-Rotating Propellers. NACA ACR No. 4B04, 1944.

TABLE I

INDEX TO FIGURES 1 TO 22

Figure	Engine power (hp)	V (mph)	D	B	σ per blade
1	300	200	8	4	0.0172, 0.0345, 0.0517, 0.069
2	300	100	6,8,10	4	0.0172, 0.0345, 0.0517, 0.069
3	300	200	6,8,10	4	0.0172, 0.0345, 0.0517, 0.069
4	300	50	6,8,10	2,4,6,8	0.0345
5	300	100	6,8,10	2,4,6,8	0.0345
6	300	150	6,8,10	2,4,6,8	0.0345
7	300	200	6,8,10	2,4,6,8	0.0345
8	225	50	6,8,10	2,4,6,8	0.0345
9	225	100	6,8,10	2,4,6,8	0.0345
10	225	150	6,8,10	2,4,6,8	0.0345
11	225	200	6,8,10	2,4,6,8	0.0345
12	150	50	6,8,10	2,4,6,8	0.0345
13	150	100	6,8,10	2,4,6,8	0.0345
14	150	150	6,8,10	2,4,6,8	0.0345
15	150	200	6,8,10	2,4,6,8	0.0345
16	100	50	6,8,10	2,4,6,8	0.0345
17	100	100	6,8,10	2,4,6,8	0.0345
18	100	150	6,8,10	2,4,6,8	0.0345
19	100	200	6,8,10	2,4,6,8	0.0345
20	50	50	6,8,10	2,4,6,8	0.0345
21	50	100	6,8,10	2,4,6,8	0.0345
22	50	150	6,8,10	2,4,6,8	0.0345

NATIONAL ADVISORY
COMMITTEE FOR AERONAUTICS

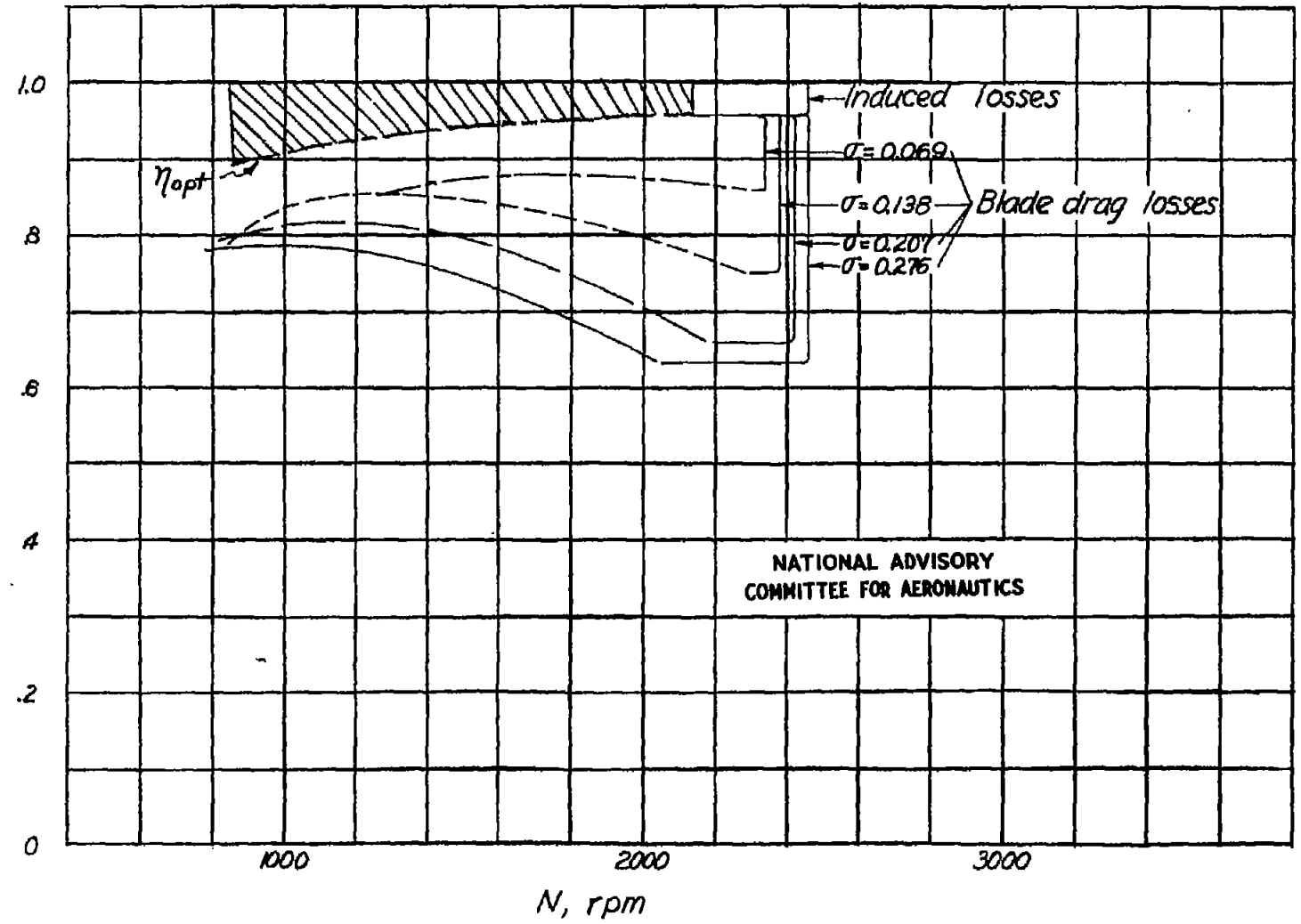

Figure 1.- Breakdown of propeller power losses. B = 4; D = 8; V = 200 miles per hour; P = 300 horsepower; η_i = 0.97.

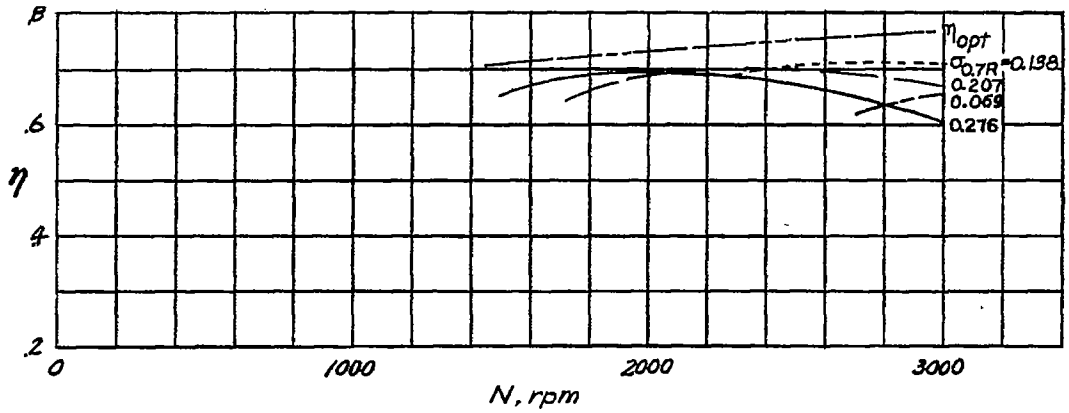

(a) D = 6.0; η_i = 0.80.

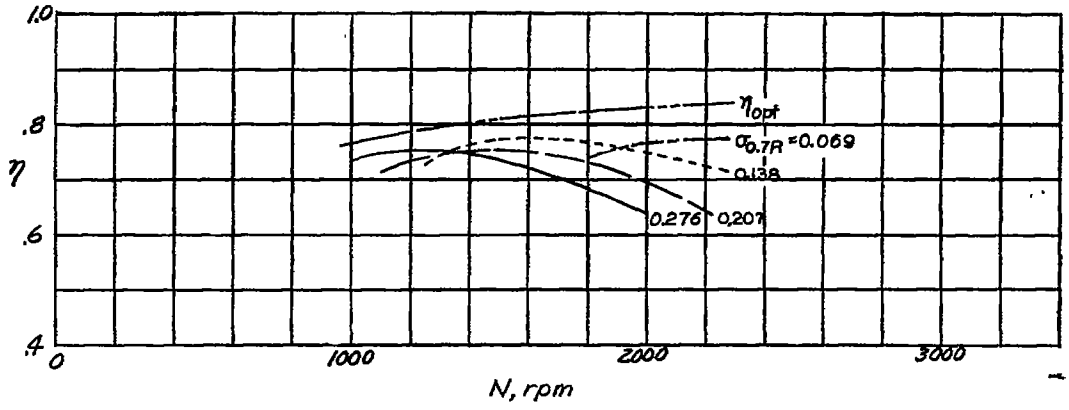

(b) D = 8.0; η_i = 0.86.

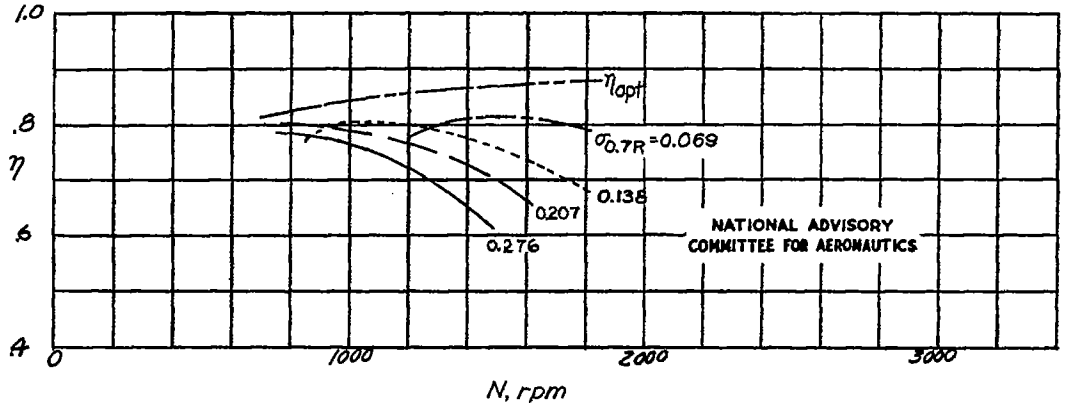

(c) D = 10.0; η_i = 0.90.

Figure 2.- Propeller efficiency. V = 100 miles per hour; P = 300 horsepower; B = 4.

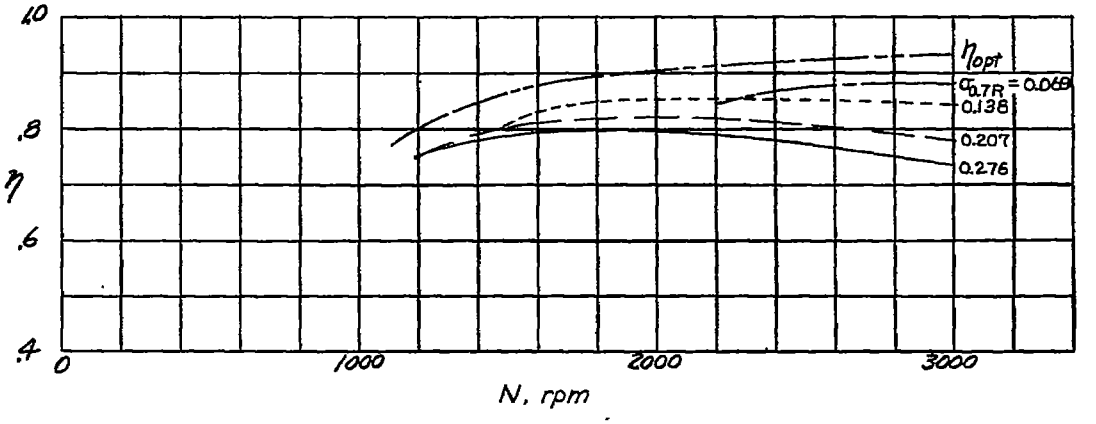

(a) D = 6.0; η_i = 0.955.

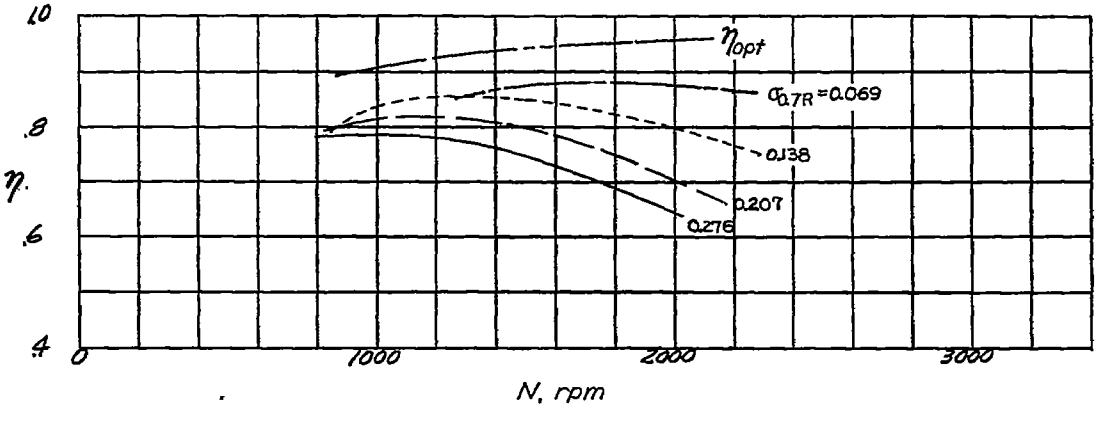

(b) D = 8.0; η_i = 0.97.

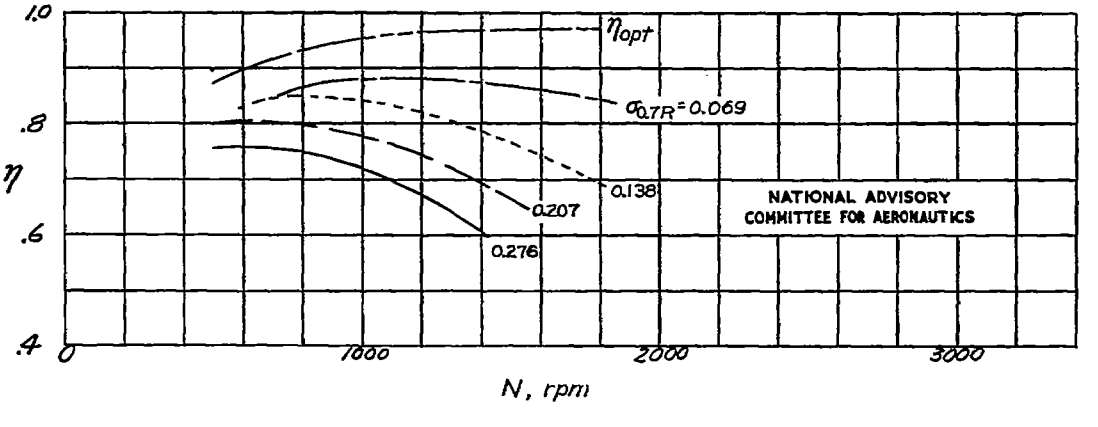

(c) D = 10.0; η_i = 0.98.

Figure 3.- Propeller efficiency. V = 200 miles per hour; P = 300 horsepower; B = 4.

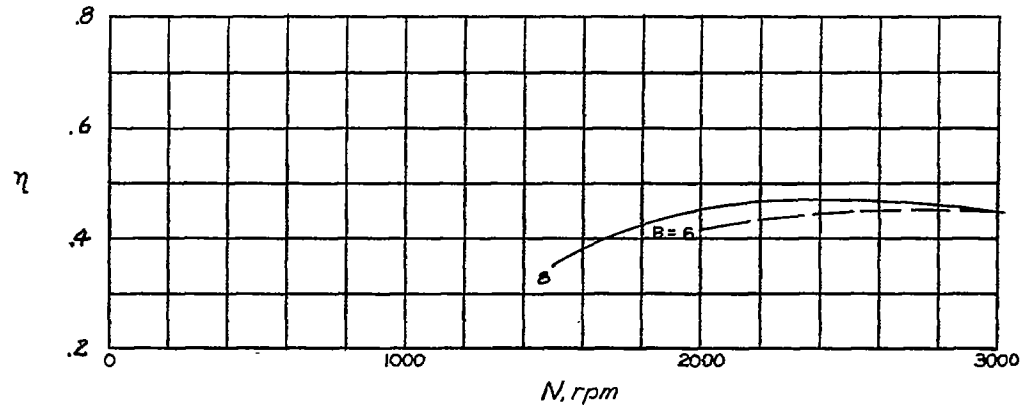

(a) D = 6.0; η_i = 0.53.

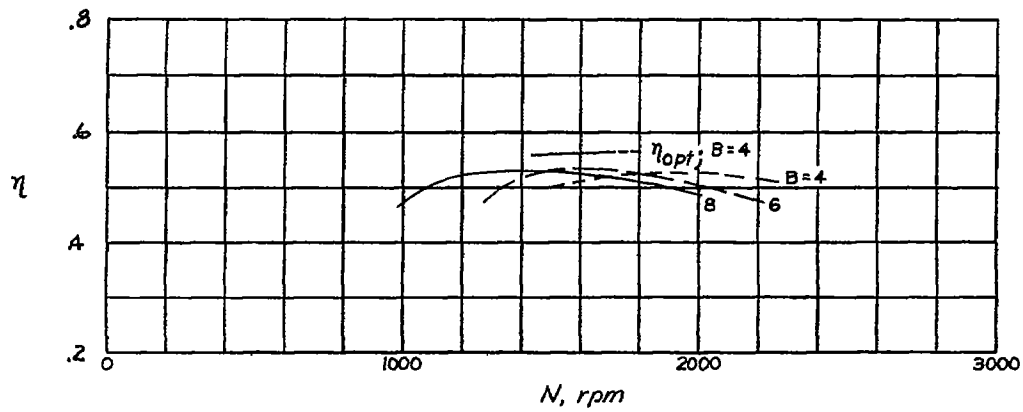

(b) D = 8.0; η_i = 0.61.

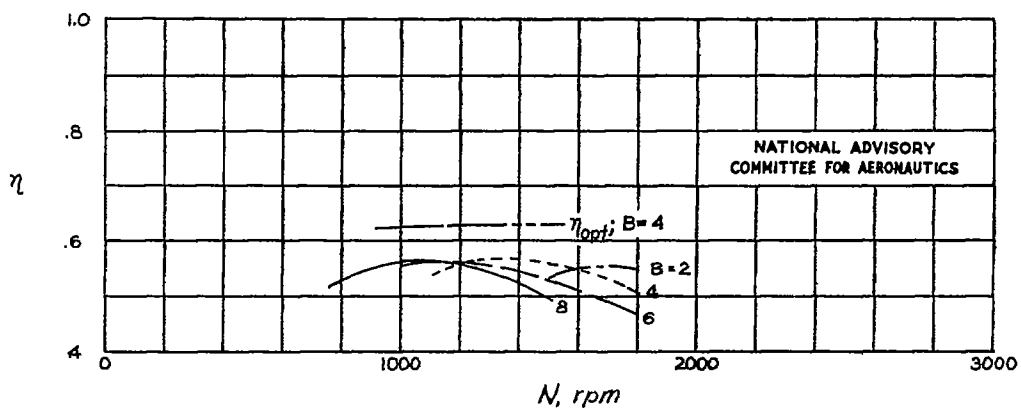

(c) D = 10.0; η_i = 0.65.

Figure 4.- Propeller efficiency. V = 50 miles per hour; P = 300 horsepower; $\sigma_{0.7R}$ = 0.0345B.

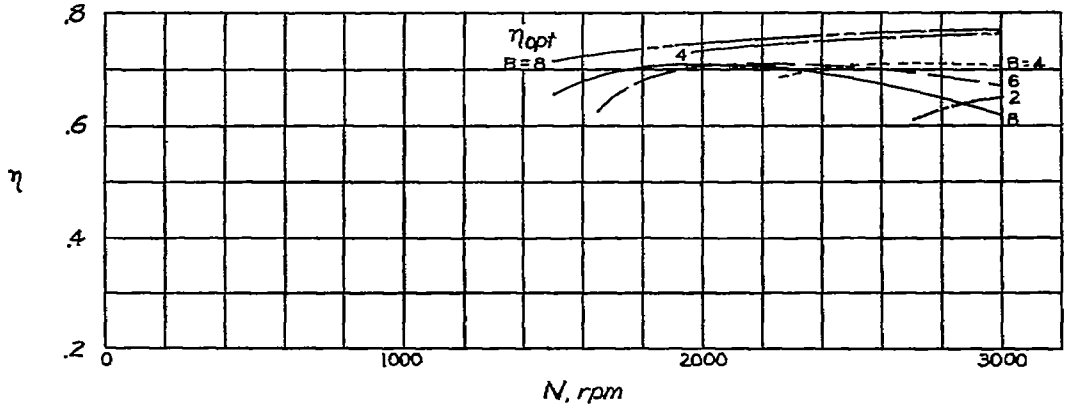

(a) D = 6.0; η_i = 0.80.

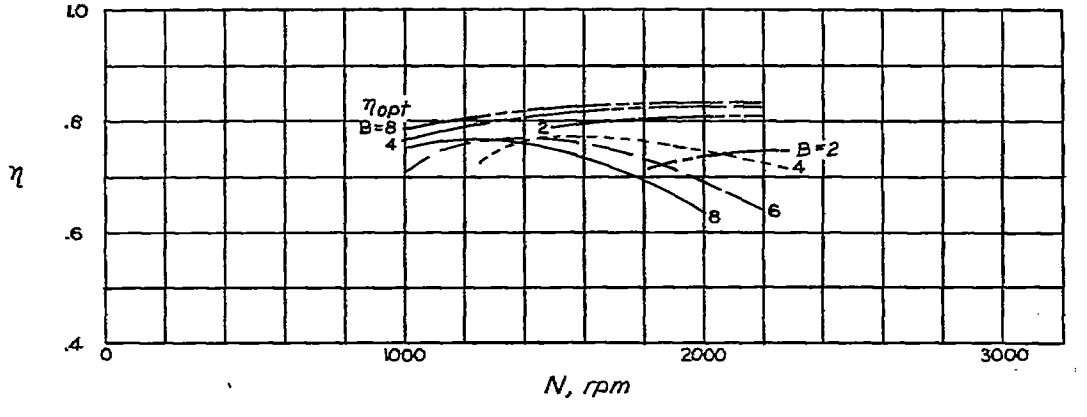

(b) D = 8.0; η_i = 0.86.

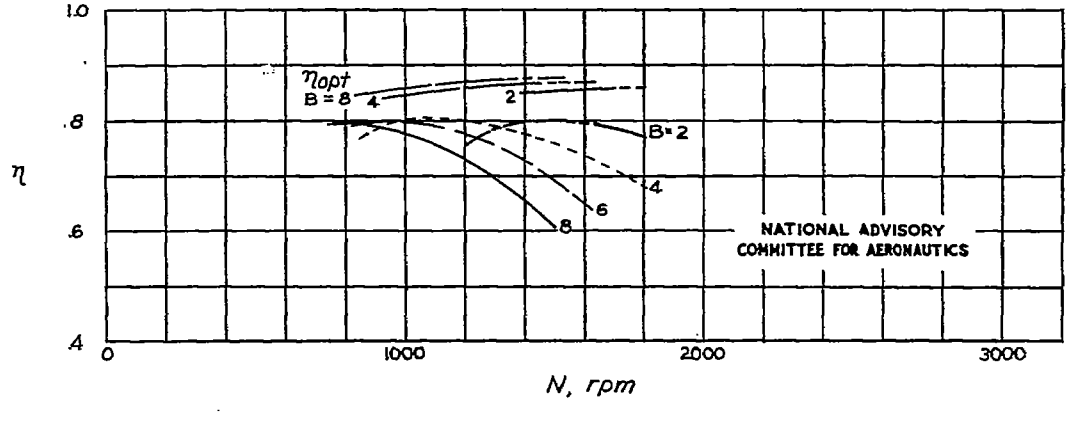

(c) D = 10.0; η_i = 0.90.

Figure 5.- Propeller efficiency. V = 100 miles per hour; P = 300 horsepower; $\sigma_{0.7R}$ = 0.0345B.

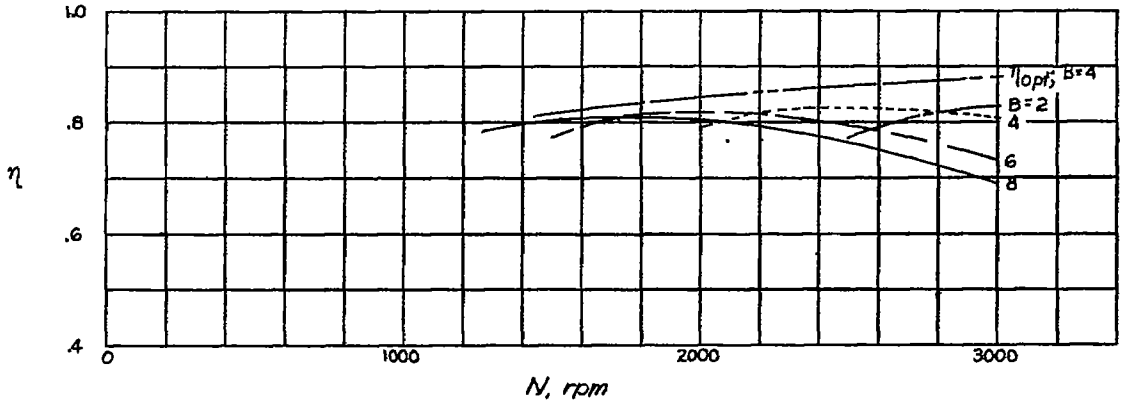

(a) D = 6.0; η_i = 0.91.

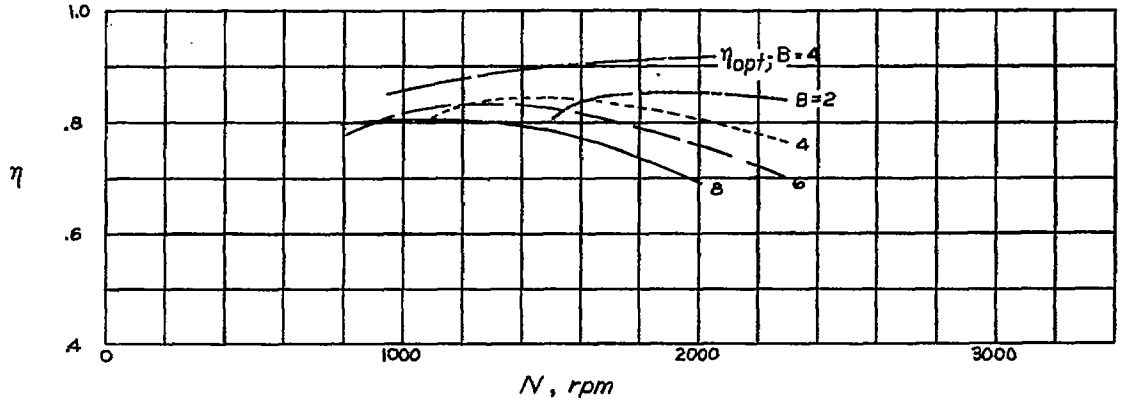

(b) D = 8.0; η_i = 0.945.

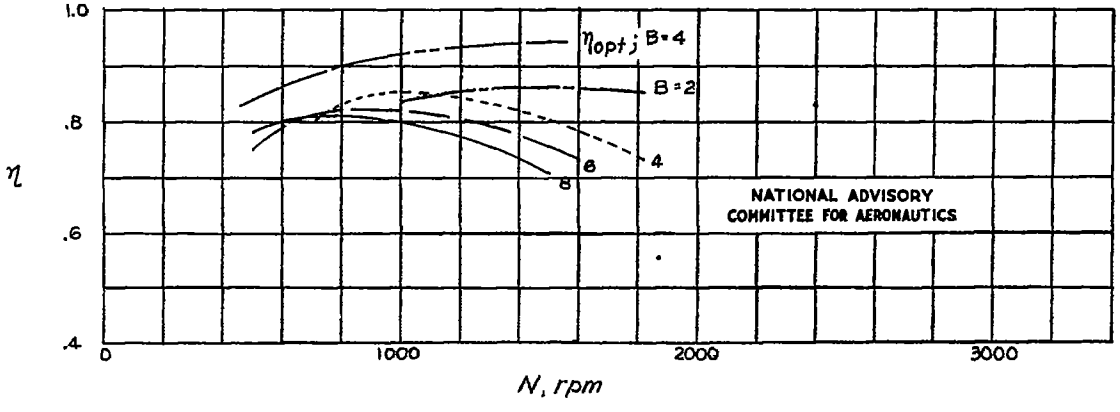

(c) D = 10.0; η_i = 0.96.

Figure 6.- Propeller efficiency. V = 150 miles per hour; P = 300 horsepower; $\sigma_{0.7R}$ = 0.0345B.

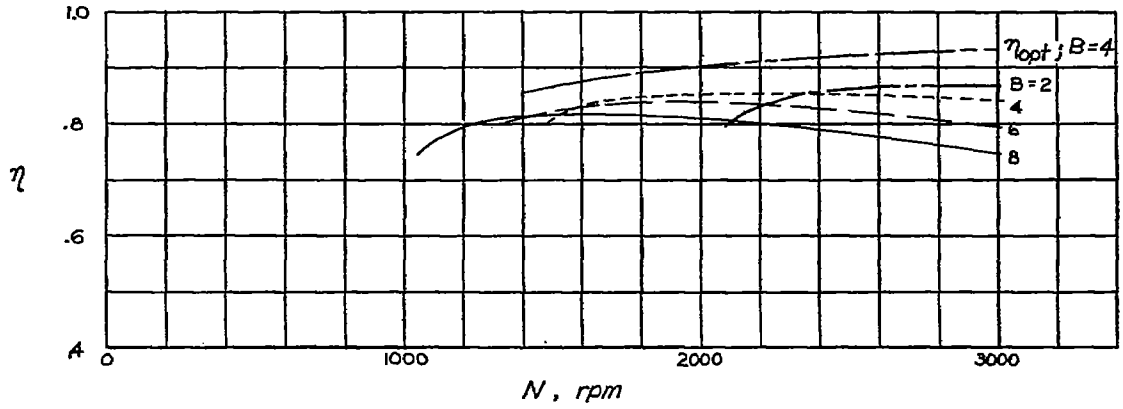

(a) D = 6.0; η_1 = 0.955.

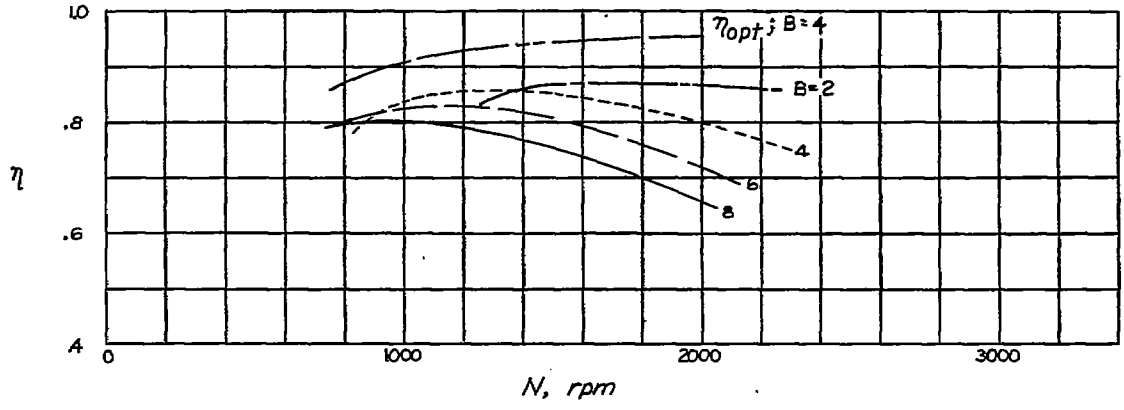

(b) D = 8.0; η_1 = 0.97.

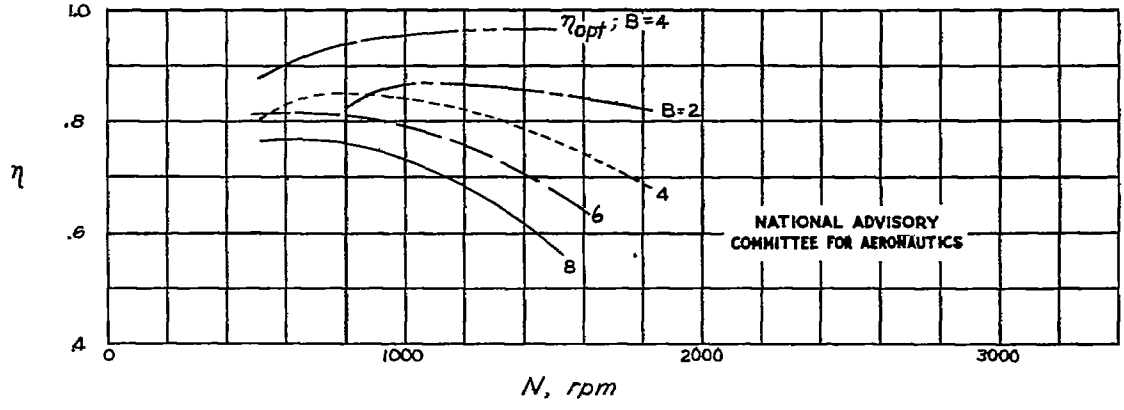

(c) D = 10.0; η_1 = 0.98.

Figure 7.- Propeller efficiency. V = 200 miles per hour; P = 300 horsepower; $\sigma_{0.7R}$ = 0.0345B.

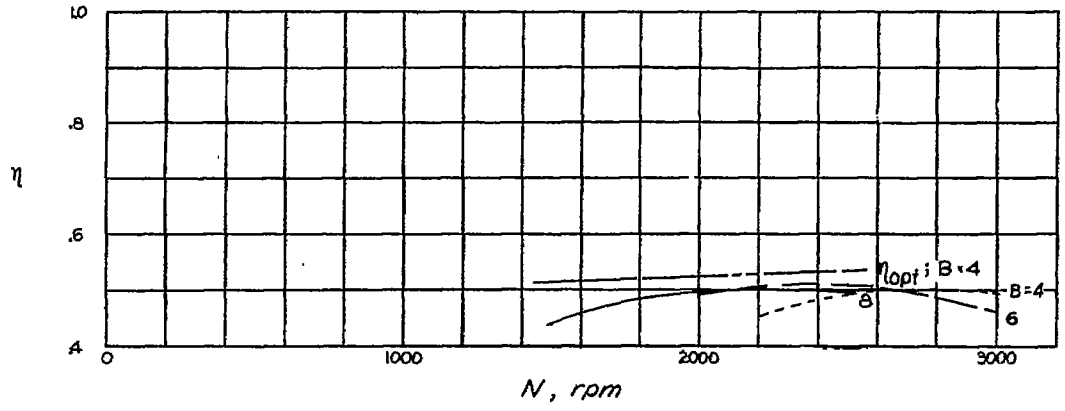

(a) D = 6.0; η_i = 0.57.

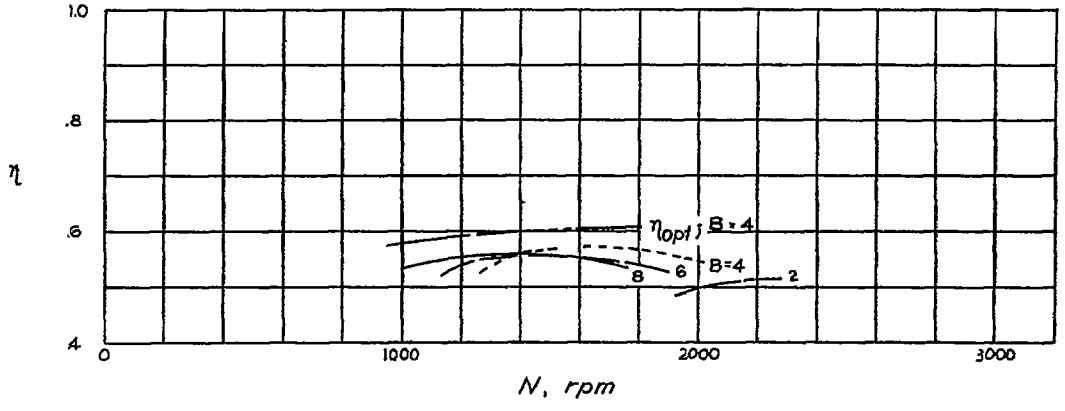

(b) D = 8.0; η_i = 0.65.

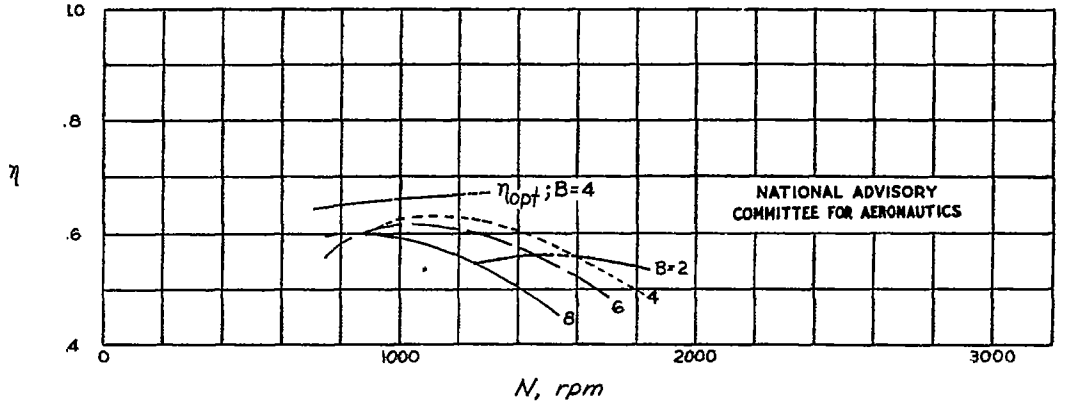

(c) D = 10.0; η_i = 0.71.

Figure 8.- Propeller efficiency. V = 50 miles per hour; P = 225 horsepower; $\sigma_{0.7R}$ = 0.0345B.

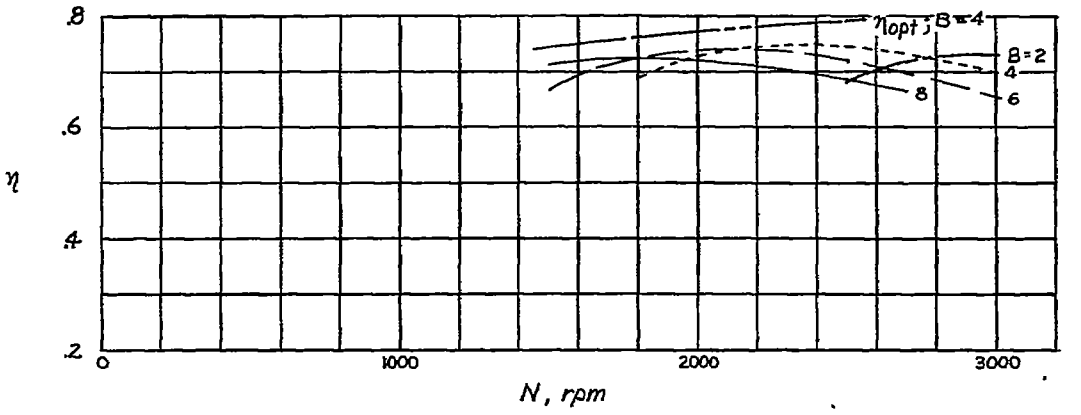

(a) D = 6.0; η_i = 0.83.

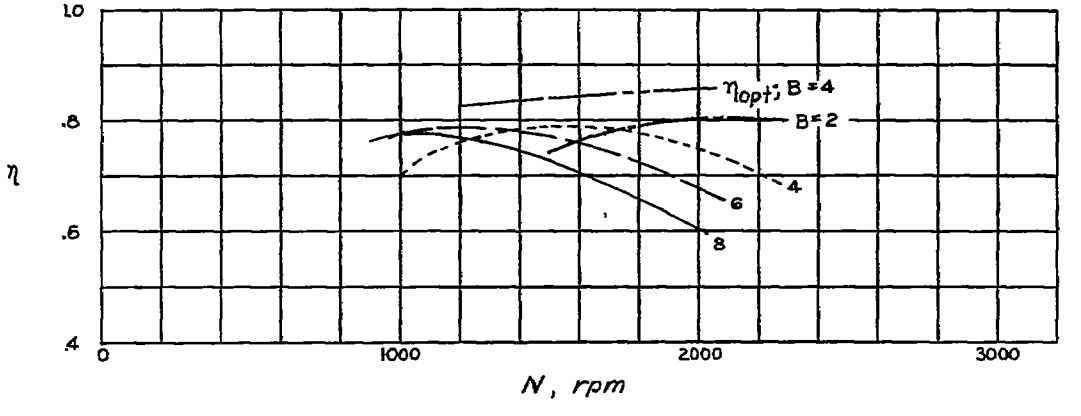

(b) D = 8.0; η_i = 0.89.

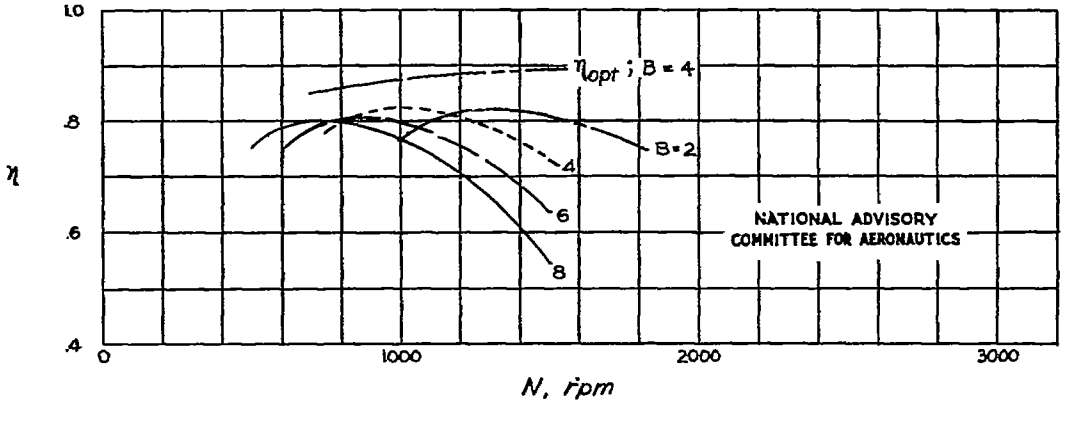

(c) D = 10.0; η_i = 0.92.

Figure 9.- Propeller efficiency. V = 100 miles per hour; P = 225 horsepower; $\sigma_{0.7R}$ = 0.0345B.

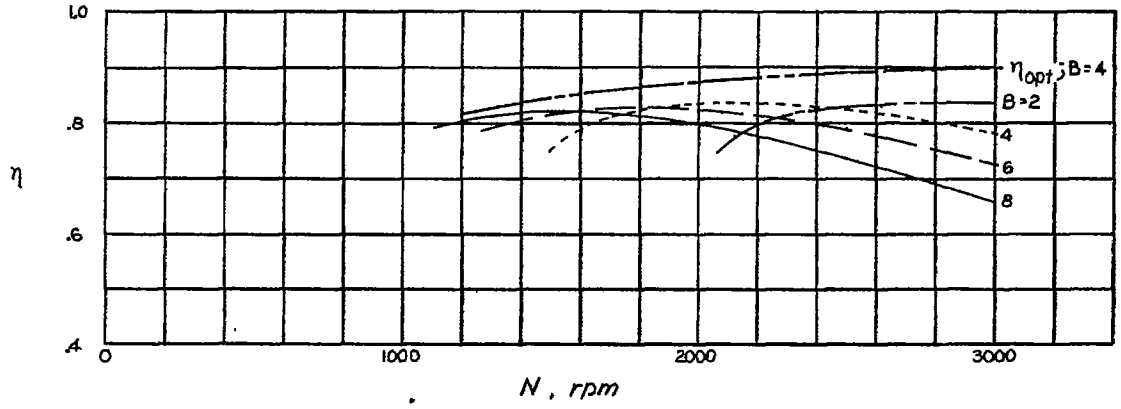

(a) D = 6.0; η_i = 0.93.

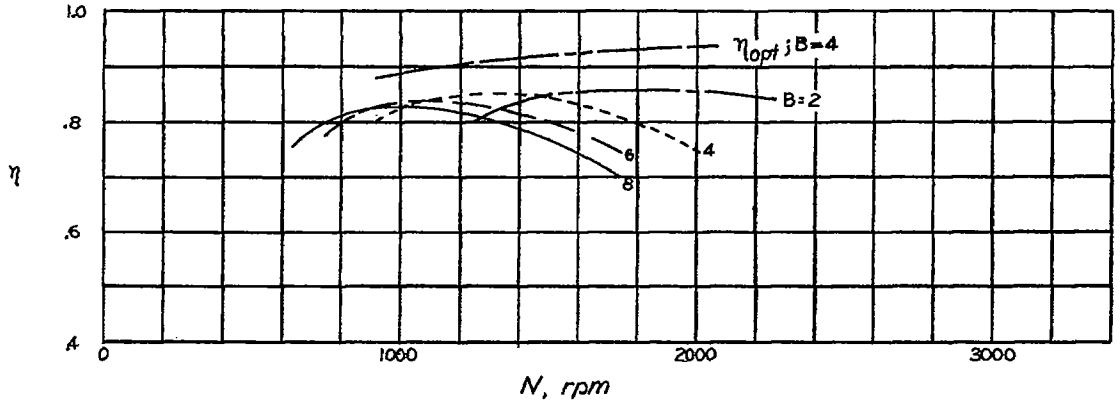

(b) D = 8.0; η_i = 0.955.

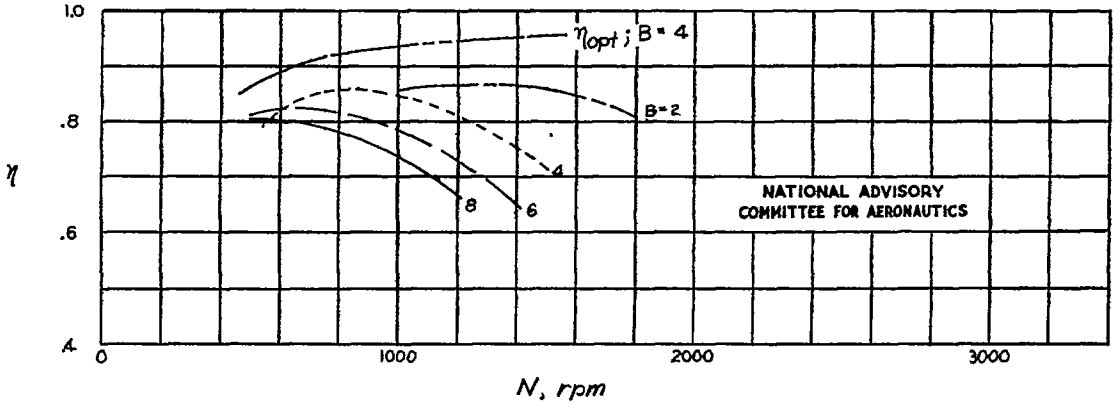

(c) D = 10.0; η_i = 0.97.

Figure 10.- Propeller efficiency. V = 150 miles per hour; P = 225 horsepower; $\sigma_{0.7R}$ = 0.0345B.

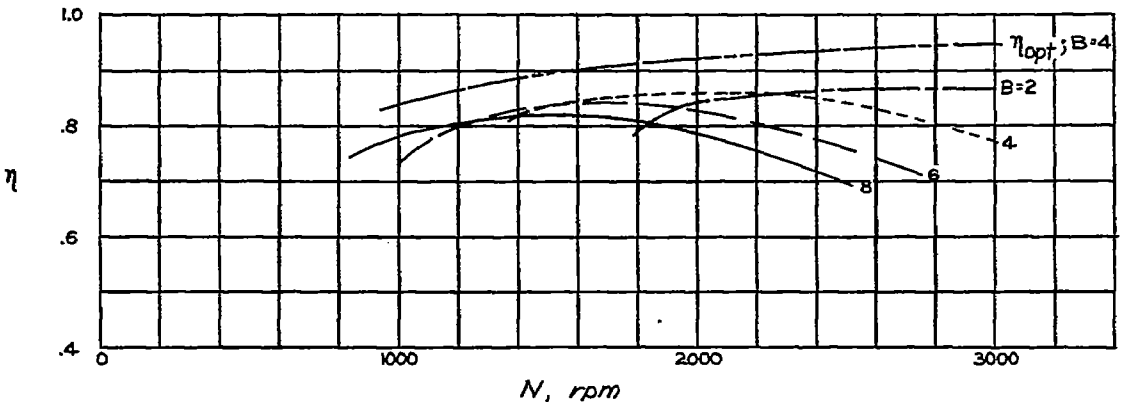

(a) D = 6.0; η_i = 0.97.

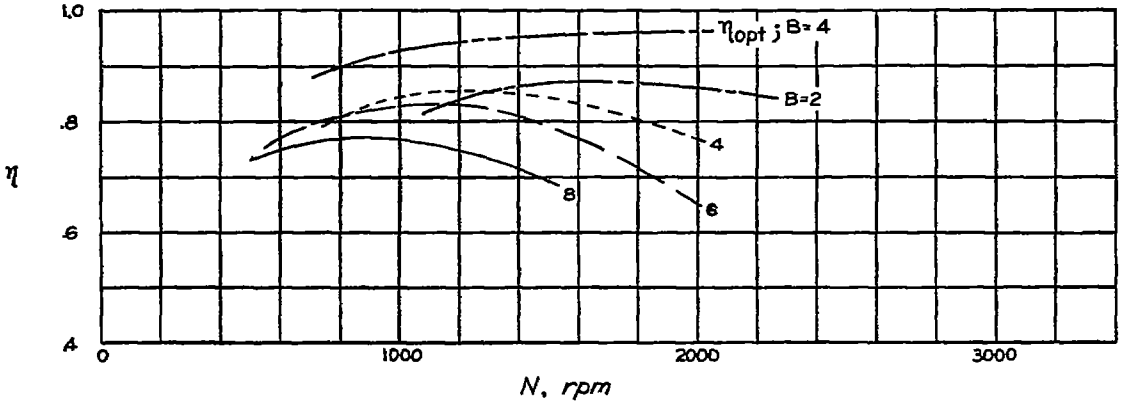

(b) D = 8.0; η_i = 0.98.

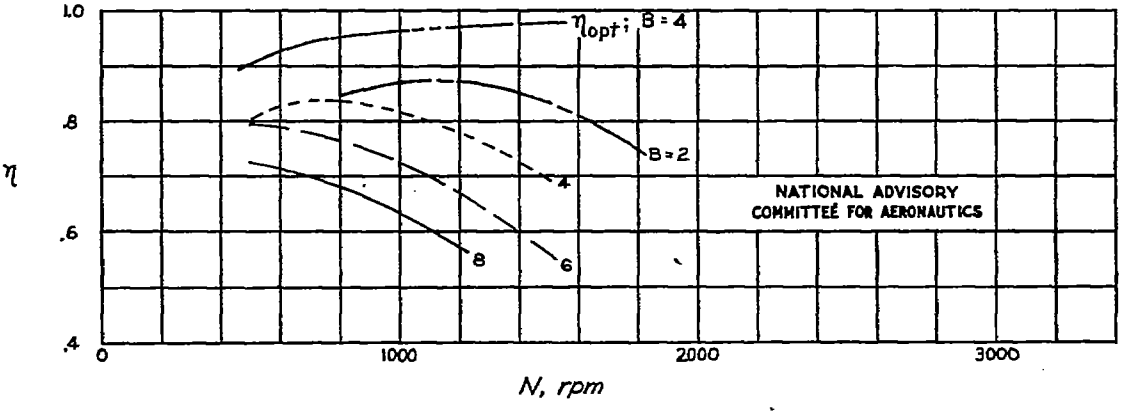

(c) D = 10.0; η_i = 0.985.

Figure 11.- Propeller efficiency. V = 200 miles per hour; P = 225 horsepower; $\sigma_{0.7R}$ = 0.0345B.

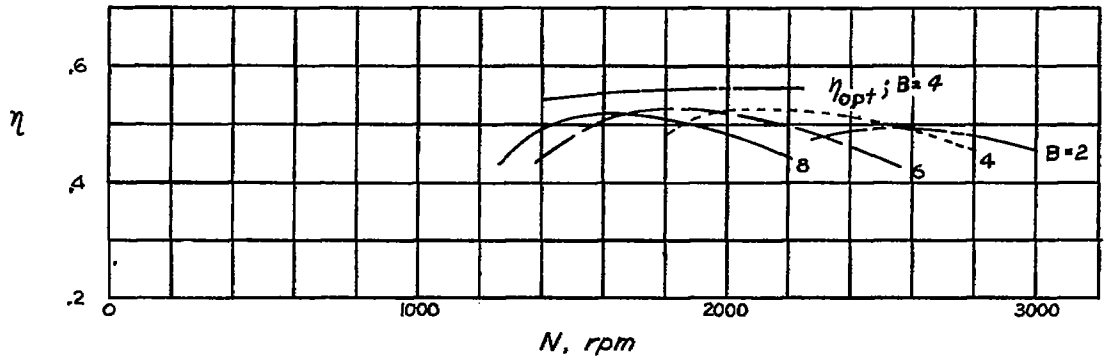

(a) D = 6.0; η_i = 0.625.

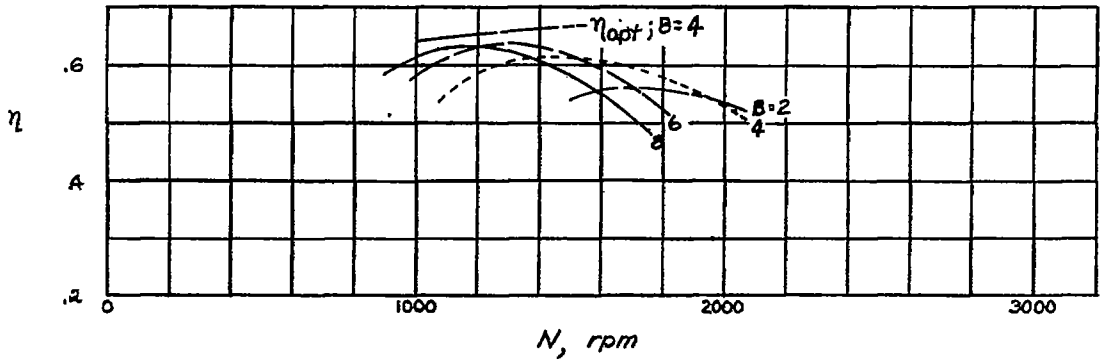

(b) D = 8.0; η_i = 0.70.

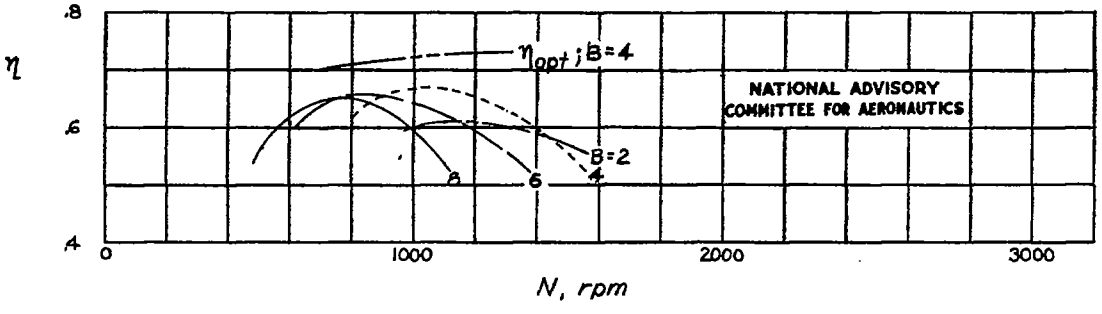

(c) D = 10.0; η_i = 0.76.

Figure 12.- Propeller efficiency. V = 50 miles per hour; P = 150 horsepower; $\sigma_{0.7R}$ = 0.0345B.

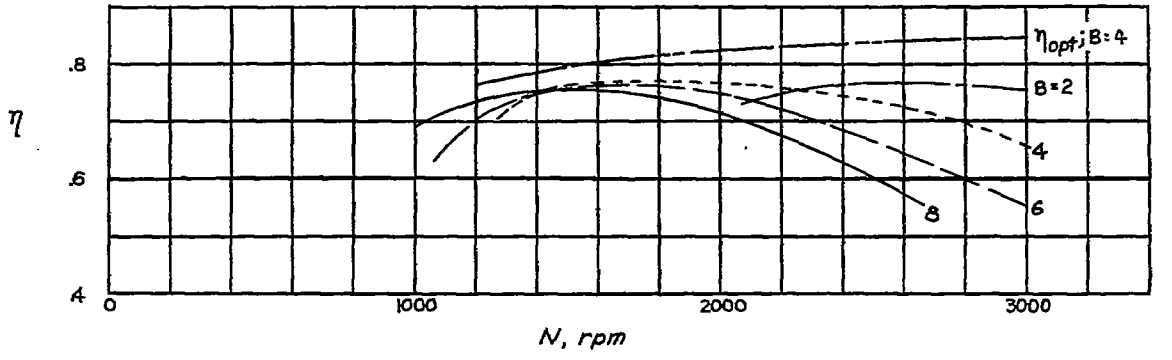

(a) D = 6.0; η_i = 0.87.

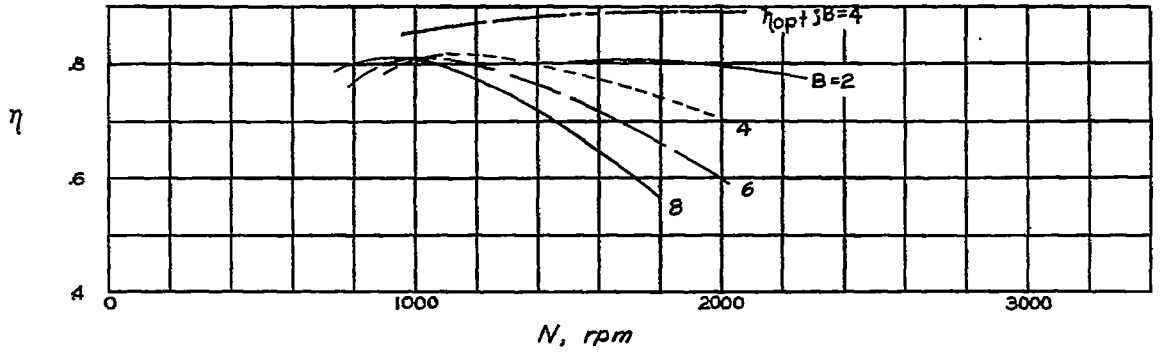

(b) D = 8.0; η_i = 0.92.

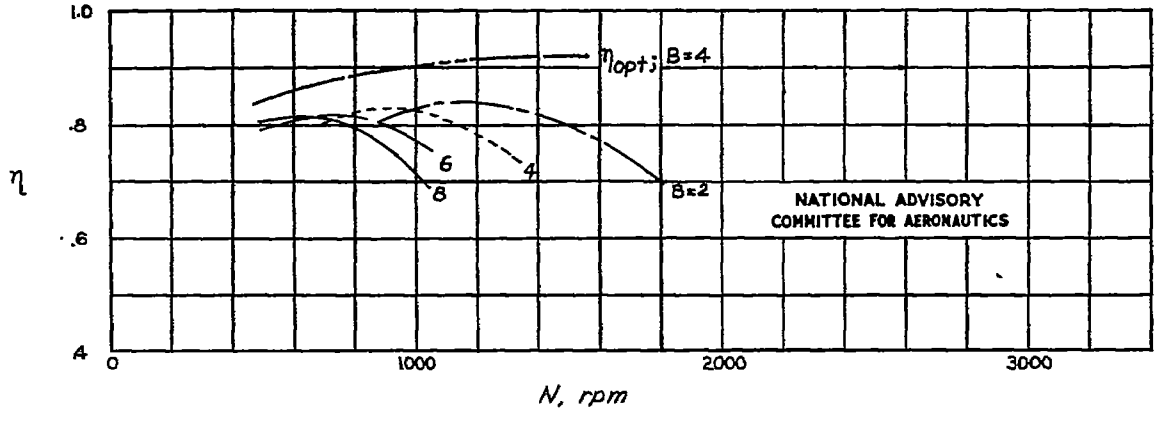

(c) D = 10.0; η_i = 0.94.

Figure 13.- Propeller efficiency. V = 100 miles per hour; P = 150 horsepower; $\sigma_{0.7R}$ = 0.0345B.

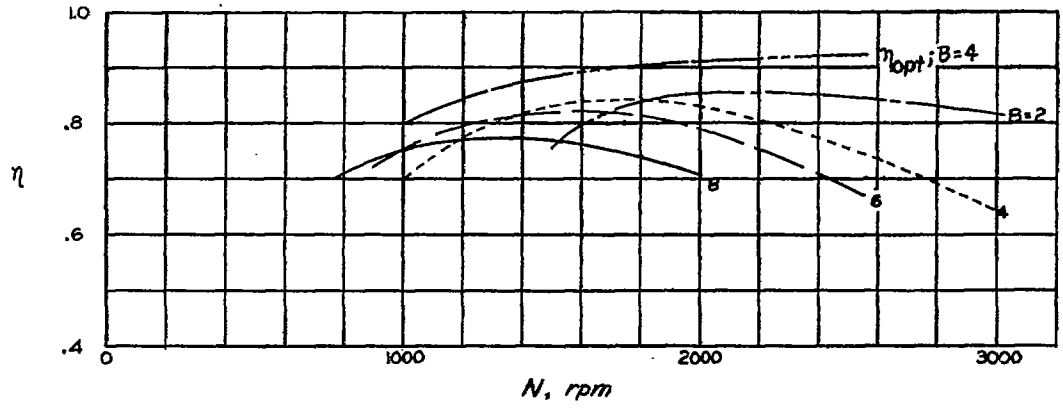

(a) D = 6.0; η_i = 0.95.

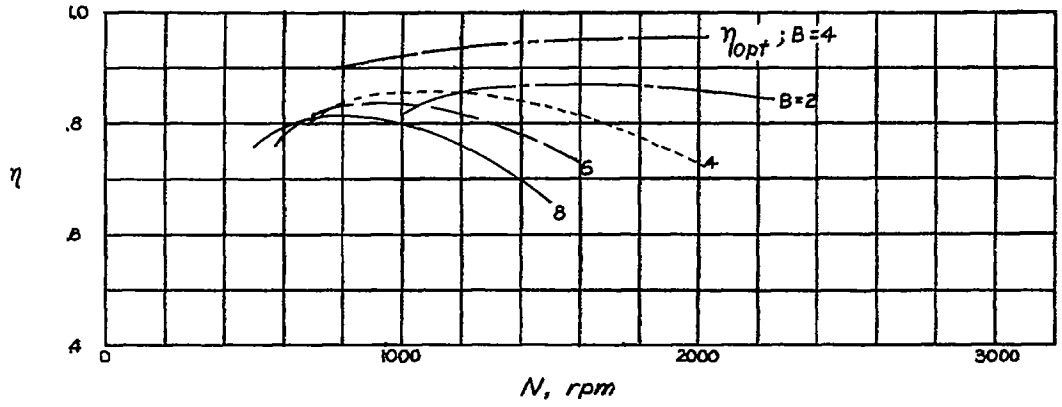

(b) D = 8.0; η_i = 0.97.

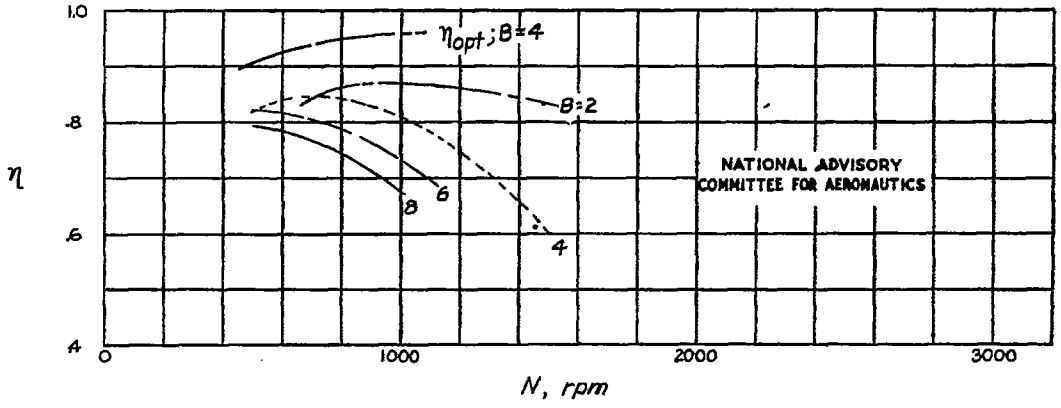

(c) D = 10.0; η_i = 0.98.

Figure 14.- Propeller efficiency. V = 150 miles per hour; P = 150 horsepower; $\sigma_{0.7R}$ = 0.0345B.

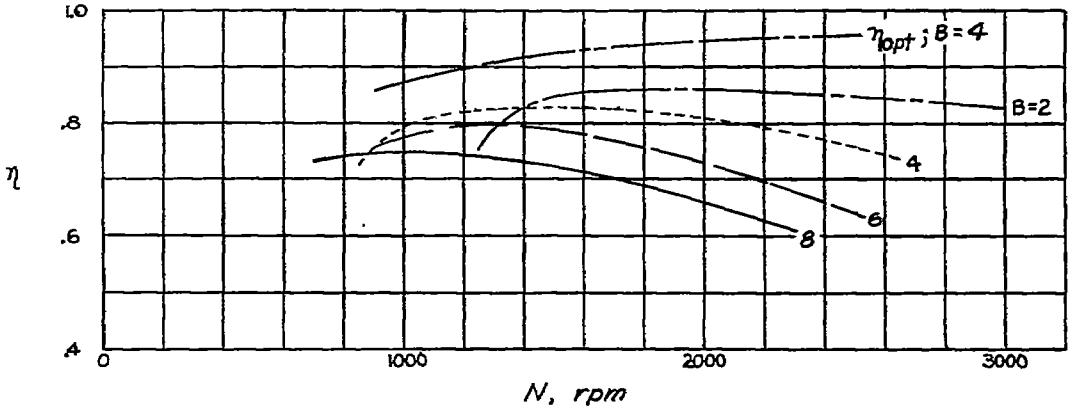

(a) D = 6.0; η_i = 0.975.

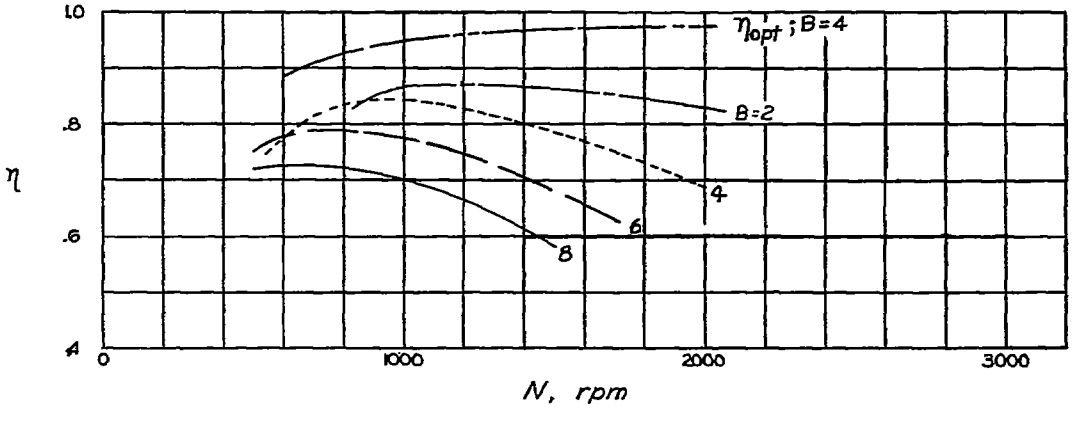

(b) D = 8.0; η_i = 0.985.

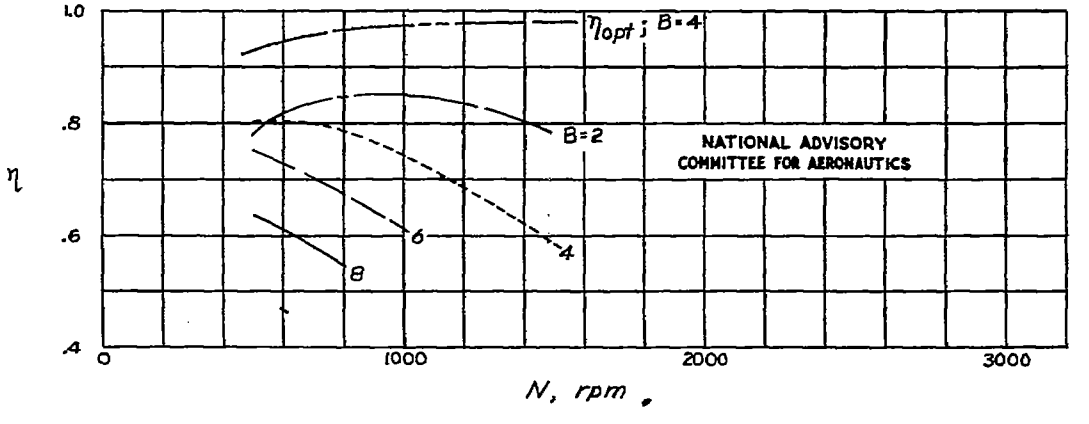

(c) D = 10.0; η_i = 0.99.

Figure 15.- Propeller efficiency. V = 200 miles per hour; P = 150 horsepower; $\sigma_{0.7R}$ = 0.0345B.

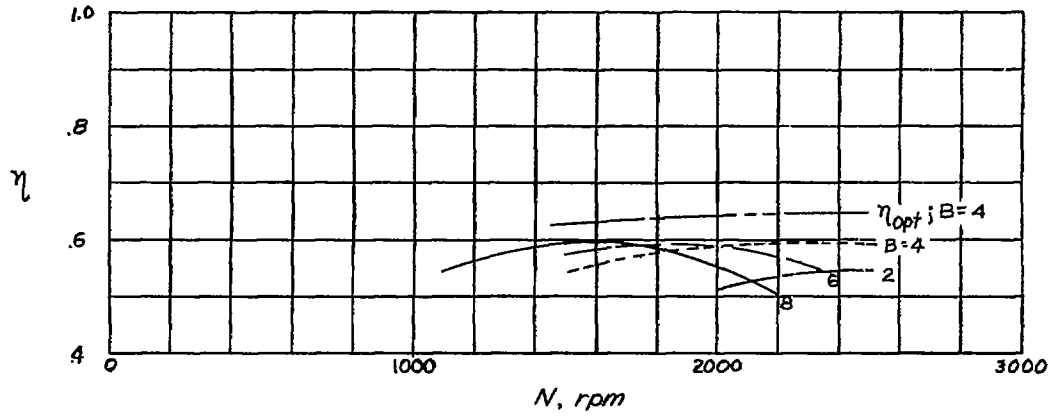

(a) D = 6.0; η_i = 0.68.

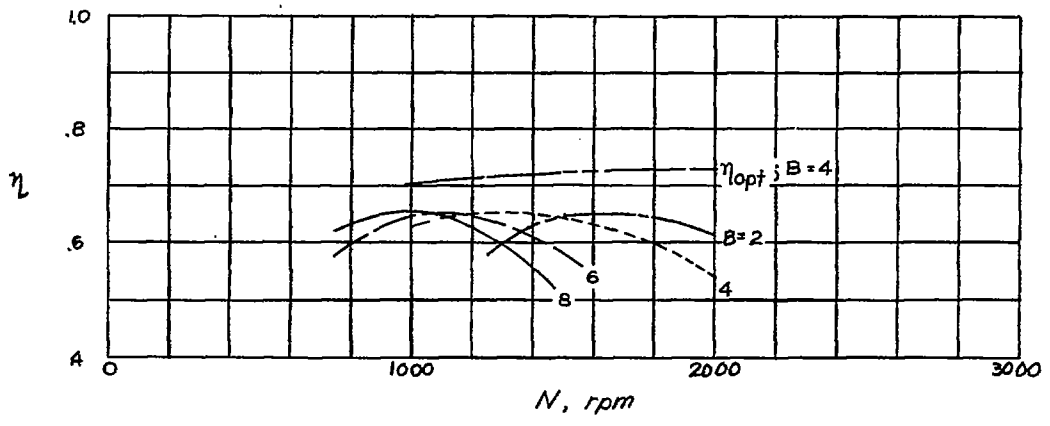

(b) D = 8.0; η_i = 0.75.

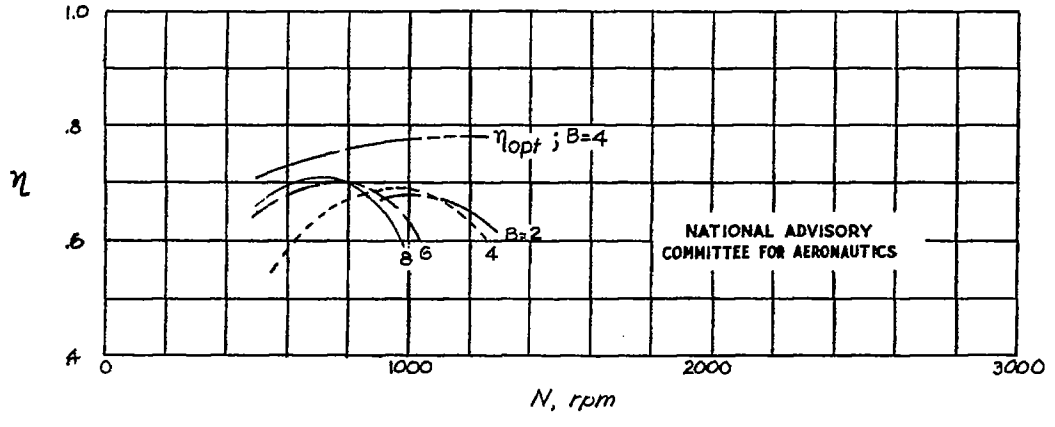

(c) D = 10.0; η_i = 0.81.

Figure 16.- Propeller efficiency. V = 50 miles per hour; P = 100 horsepower; $\sigma_{0.7R}$ = 0.0345B.

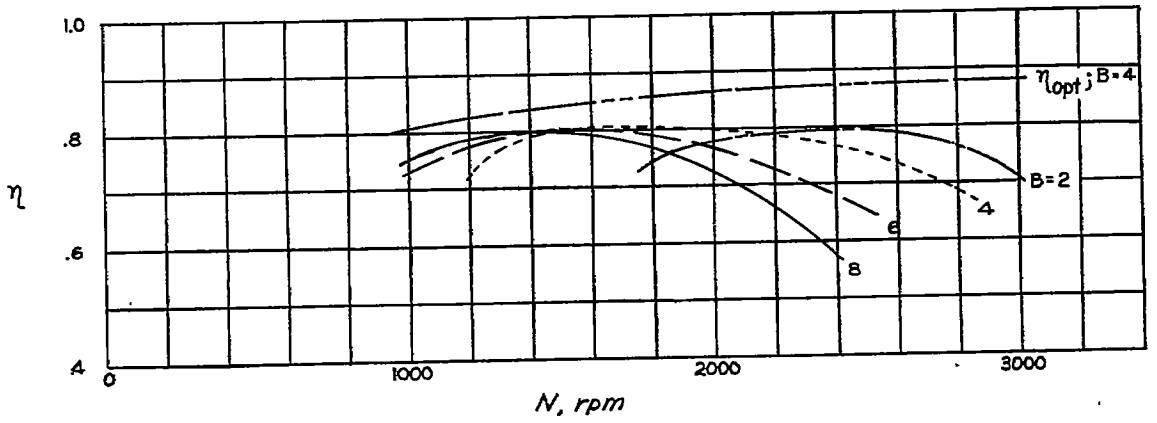

(a) D = 6.0; η_i = 0.90.

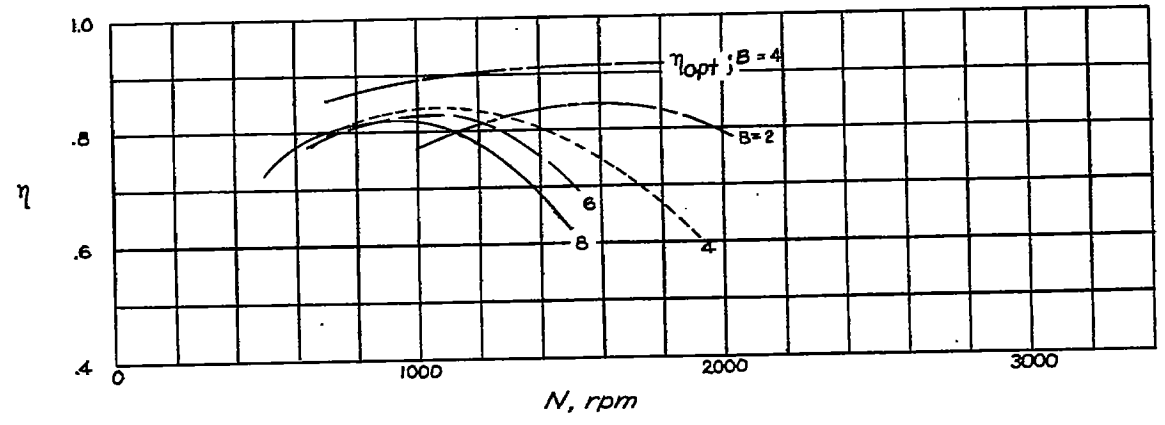

(b) D = 8.0; η_i = 0.94.

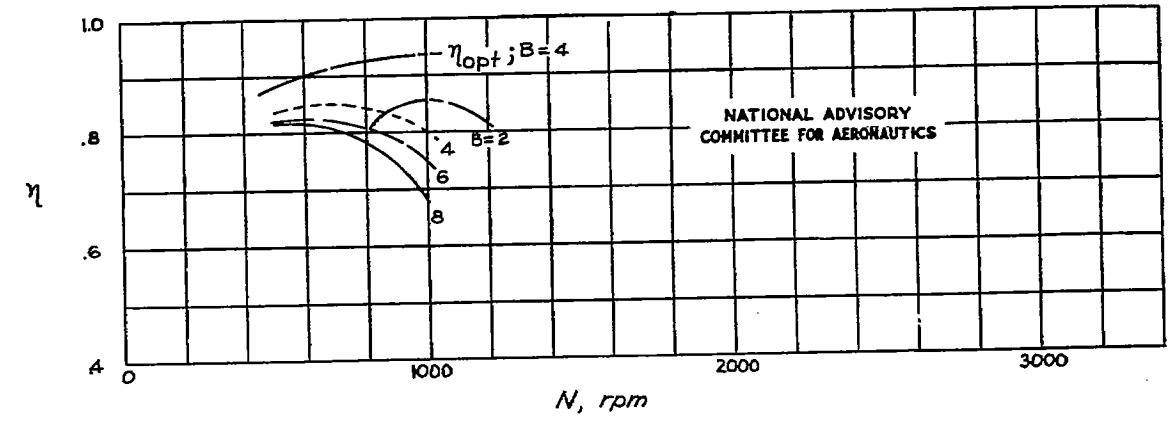

(c) D = 10.0; η_i = 0.96.

Figure 17.- Propeller efficiency. V = 100 miles per hour; P = 100 horsepower; $\sigma_{0.7R}$ = 0.0345B.

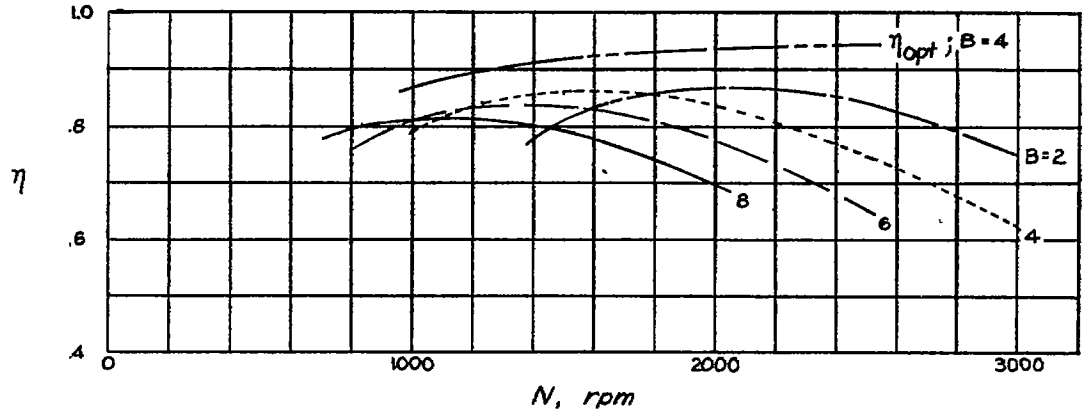

(a) D = 6.0; η_i = 0.965.

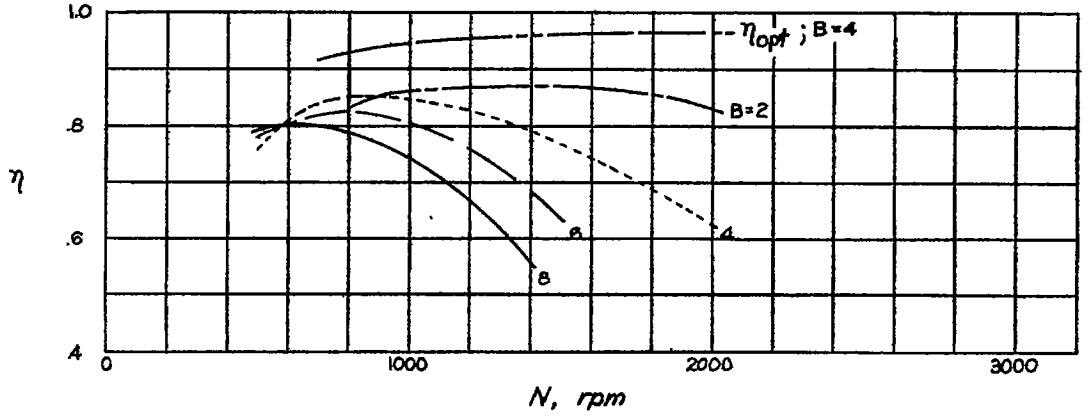

(b) D = 8.0; η_i = 0.98.

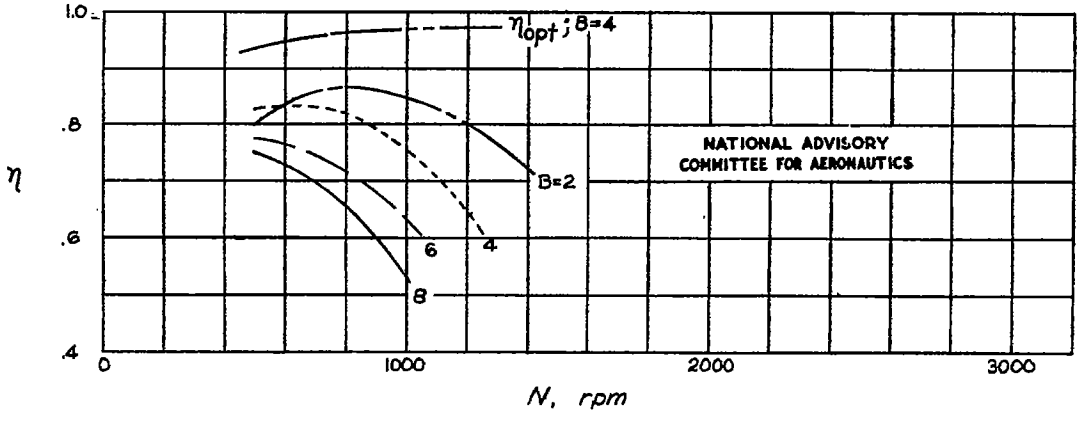

(c) D = 10.0; η_i = 0.985.

Figure 18.- Propeller efficiency. V = 150 miles per hour; P = 100 horsepower; $\sigma_{0.7R}$ = 0.0345B.

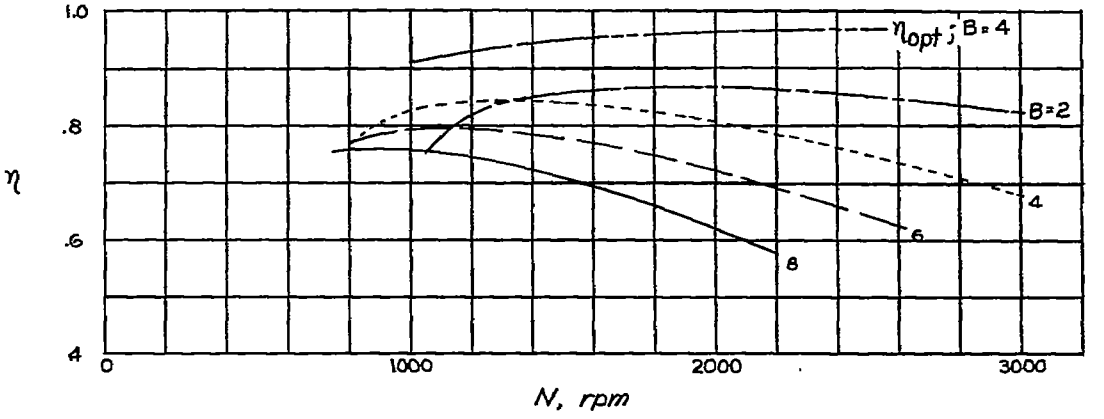

(a) D = 6.0; η_i = 0.985.

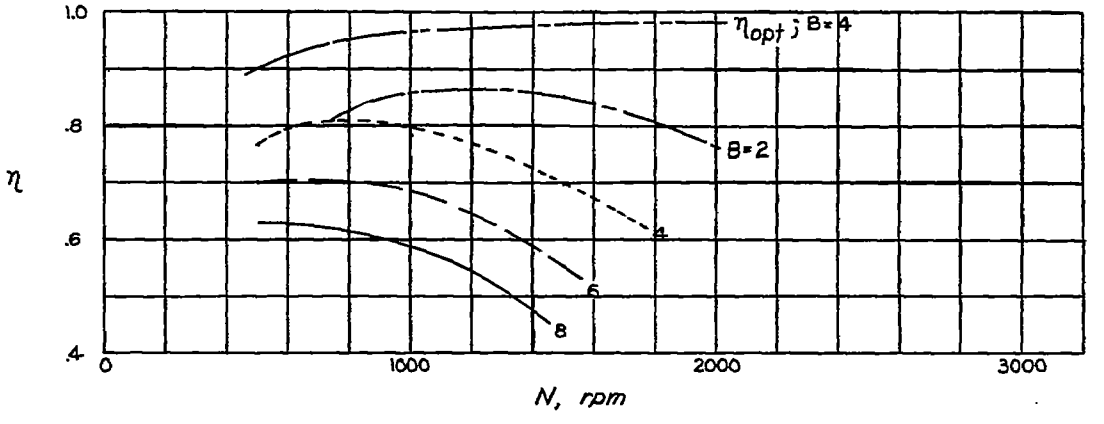

(b) D = 8.0; η_i = 0.99.

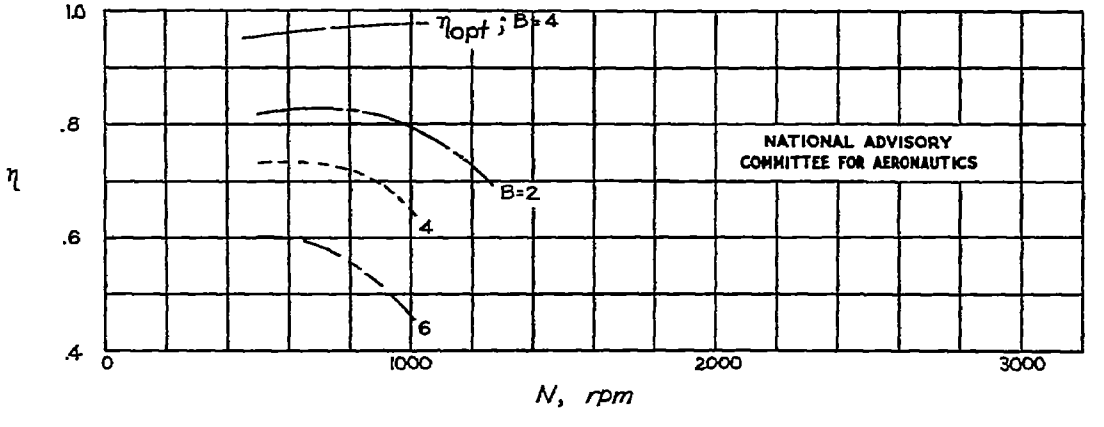

(c) D = 10.0; η_i = 0.995.

Figure 19.- Propeller efficiency. V = 200 miles per hour; P = 100 horsepower; $\sigma_{0.7R}$ = 0.0345B.

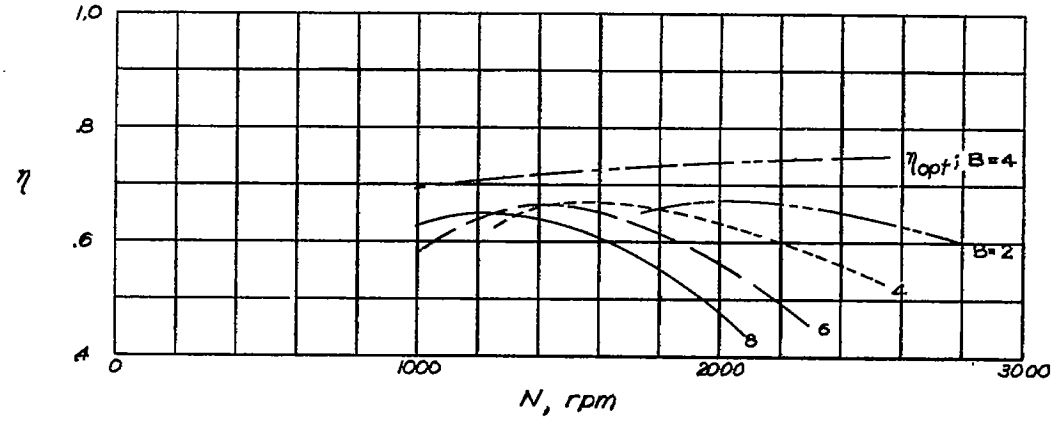

(a) D = 6.0; η_i = 0.765.

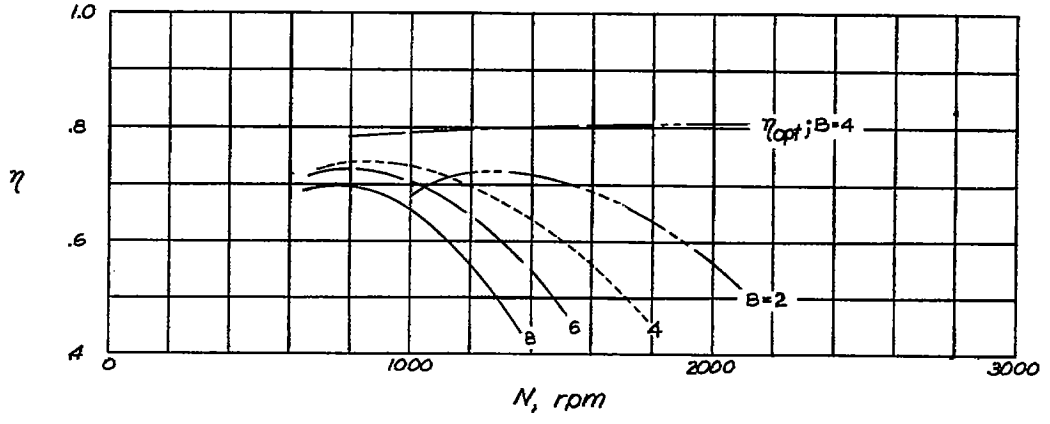

(b) D = 8.0; η_i = 0.835.

NATIONAL ADVISORY
COMMITTEE FOR AERONAUTICS

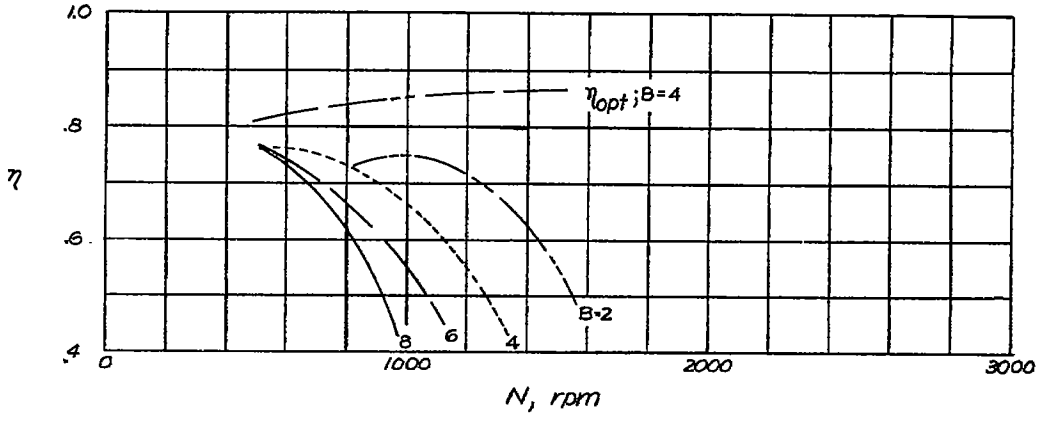

(c) D = 10.0; η_i = 0.875.

Figure 20.- Propeller efficiency. V = 50 miles per hour; P = 50 horsepower; $\sigma_{0.7R}$ = 0.0345B.

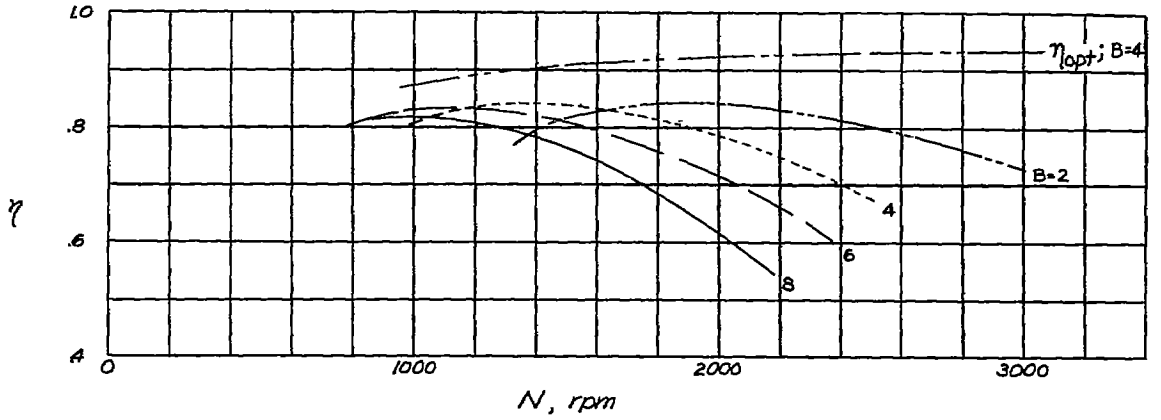

(a) D = 6.0; η_i = 0.945.

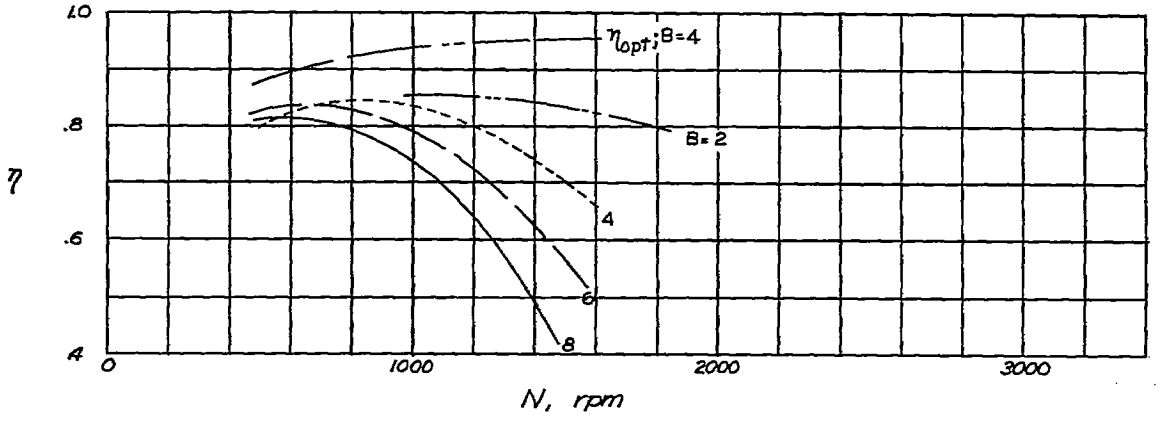

(b) D = 8.0; η_i = 0.965.

NATIONAL ADVISORY COMMITTEE FOR AERONAUTICS.

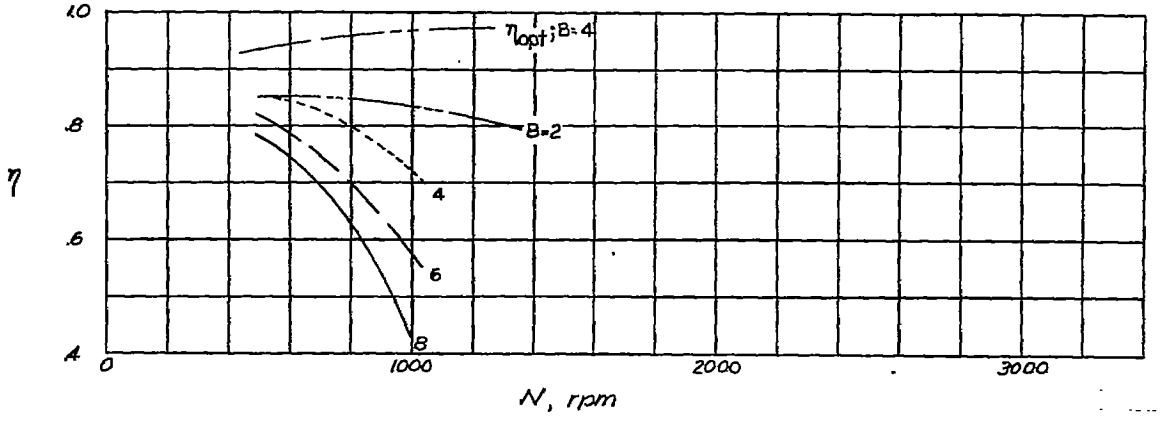

(c) D = 10.0; η_i = 0.98.

Figure 21.- Propeller efficiency. V = 100 miles per hour; P = 50 horsepower; $\sigma_{0.7R}$ = 0.0345B.

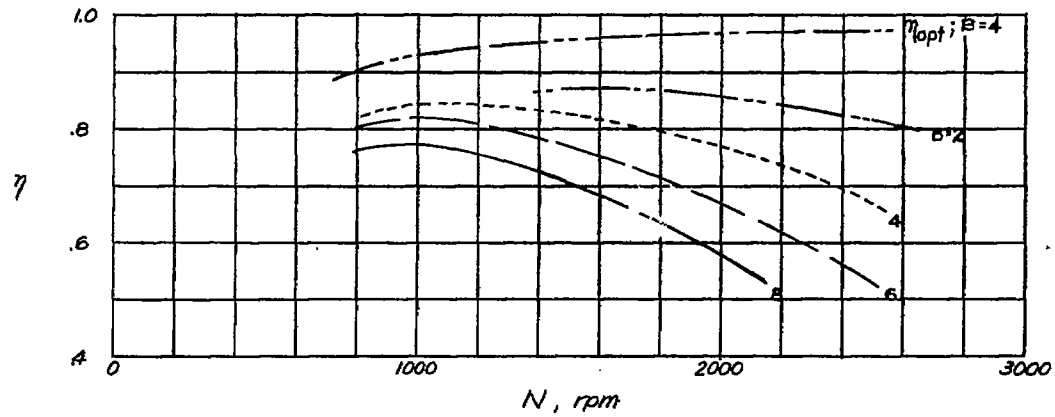

(a) D = 6.0; η_i = 0.98.

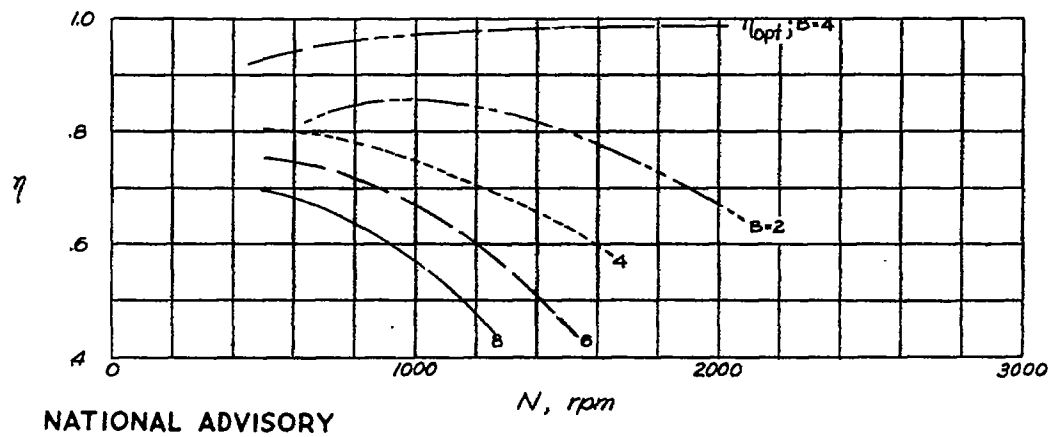

NATIONAL ADVISORY
COMMITTEE FOR AERONAUTICS

(b) D = 8.0; η_i = 0.99.

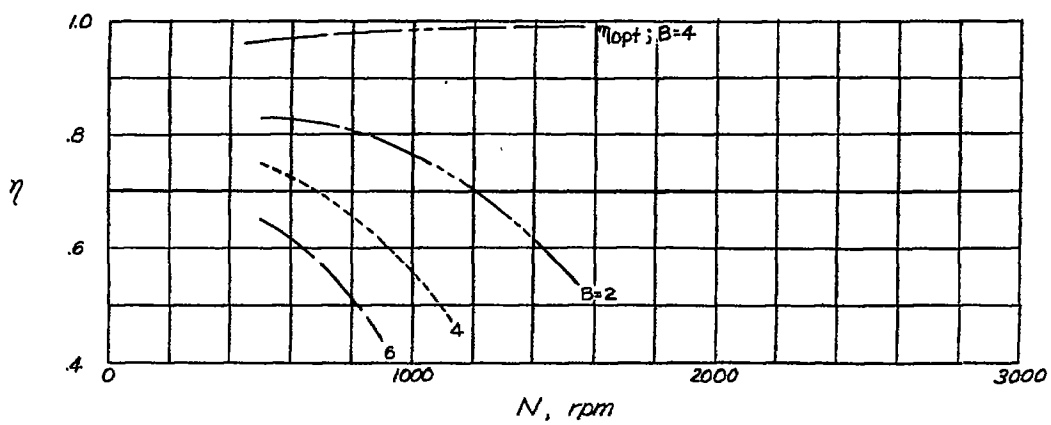

(c) D = 10.0; η_i = 0.995.

Figure 22.- Propeller efficiency. V = 150 miles per hour; P = 50 horsepower; $\sigma_{0.7R}$ = 0.03458.

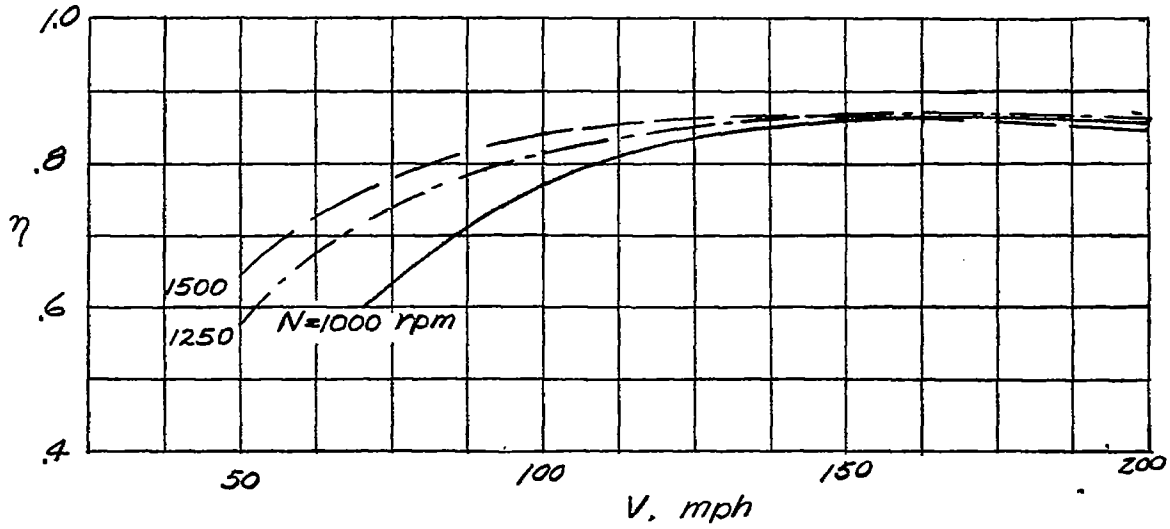

(a) D = 8.0; B = 2.

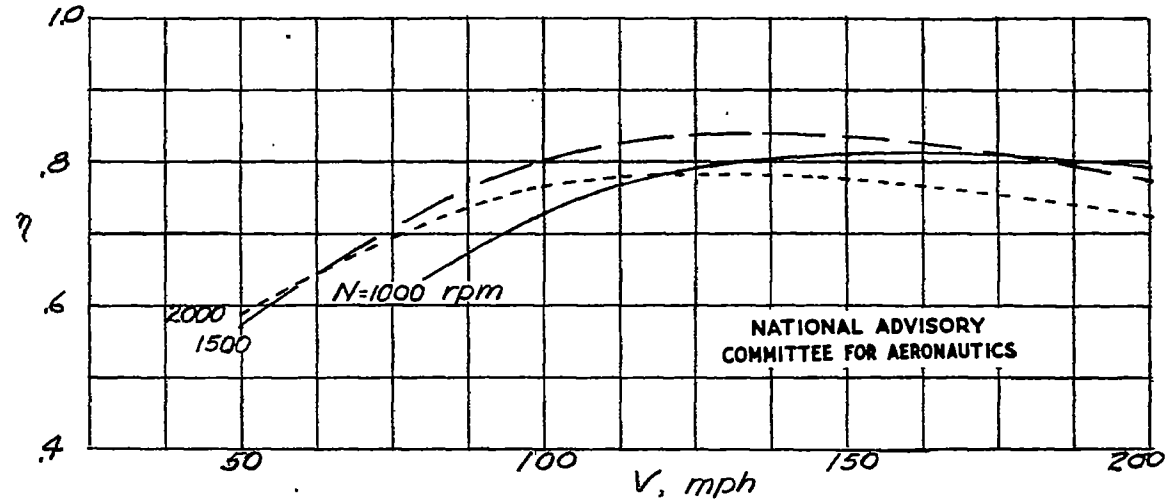

(b) D = 6.0; B = 6.

Figure 23.- Propeller efficiency. P = 100 horsepower.

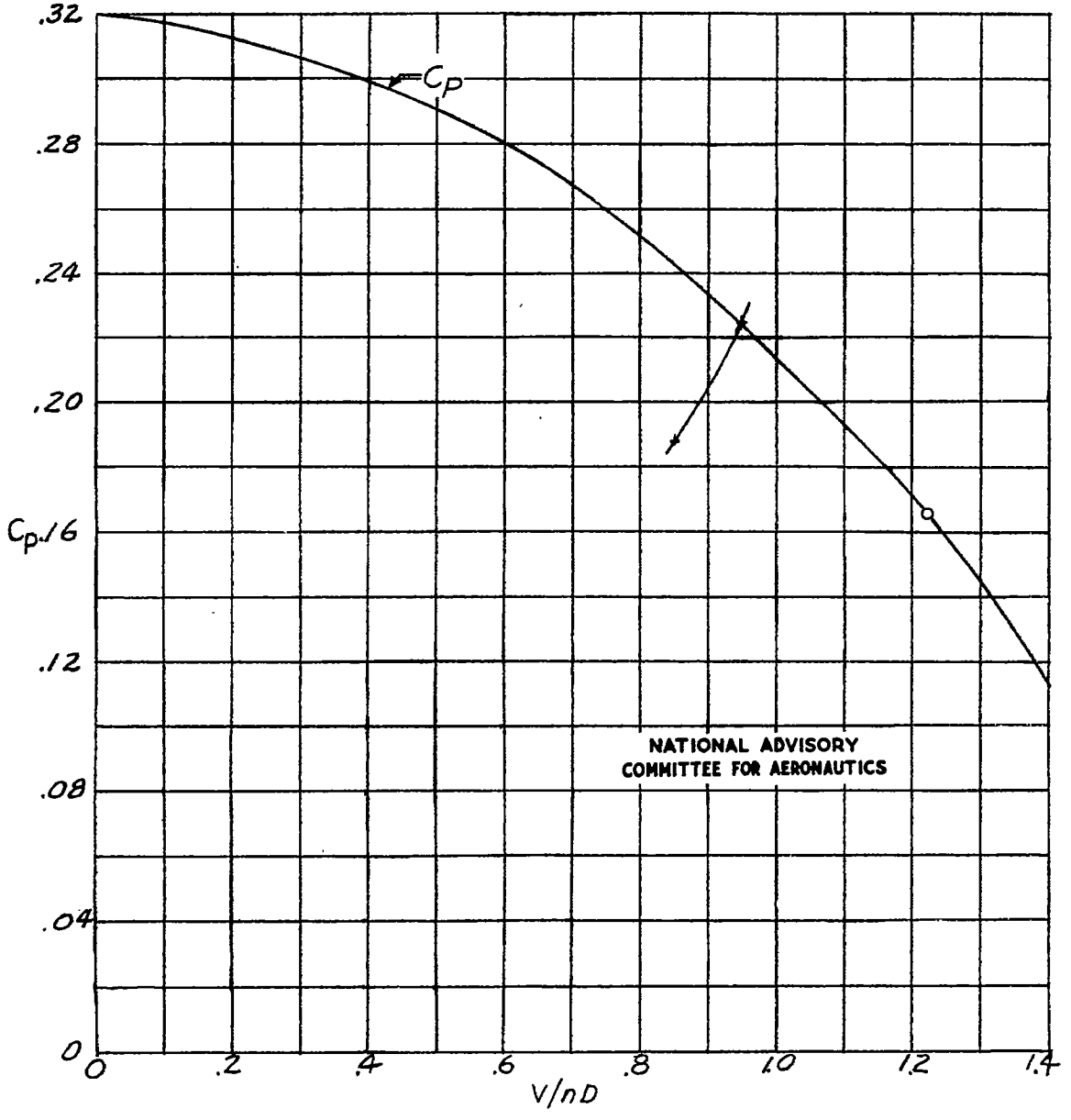

Figure 24.- Power-coefficient curve for use in fixed-pitch analysis.

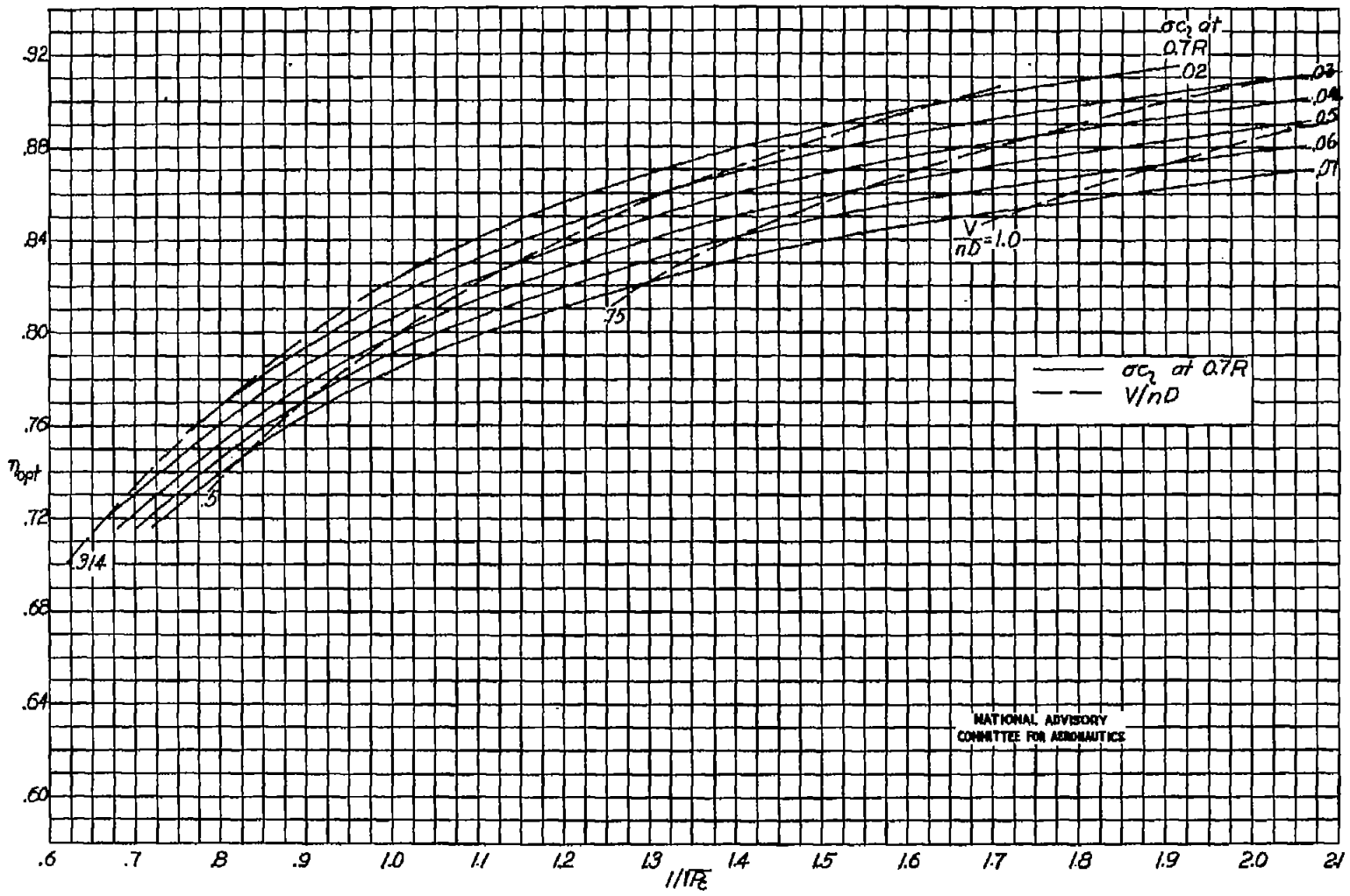

(a) Two-blade propellers.

Figure 25.- Propeller performance chart. Without drag.

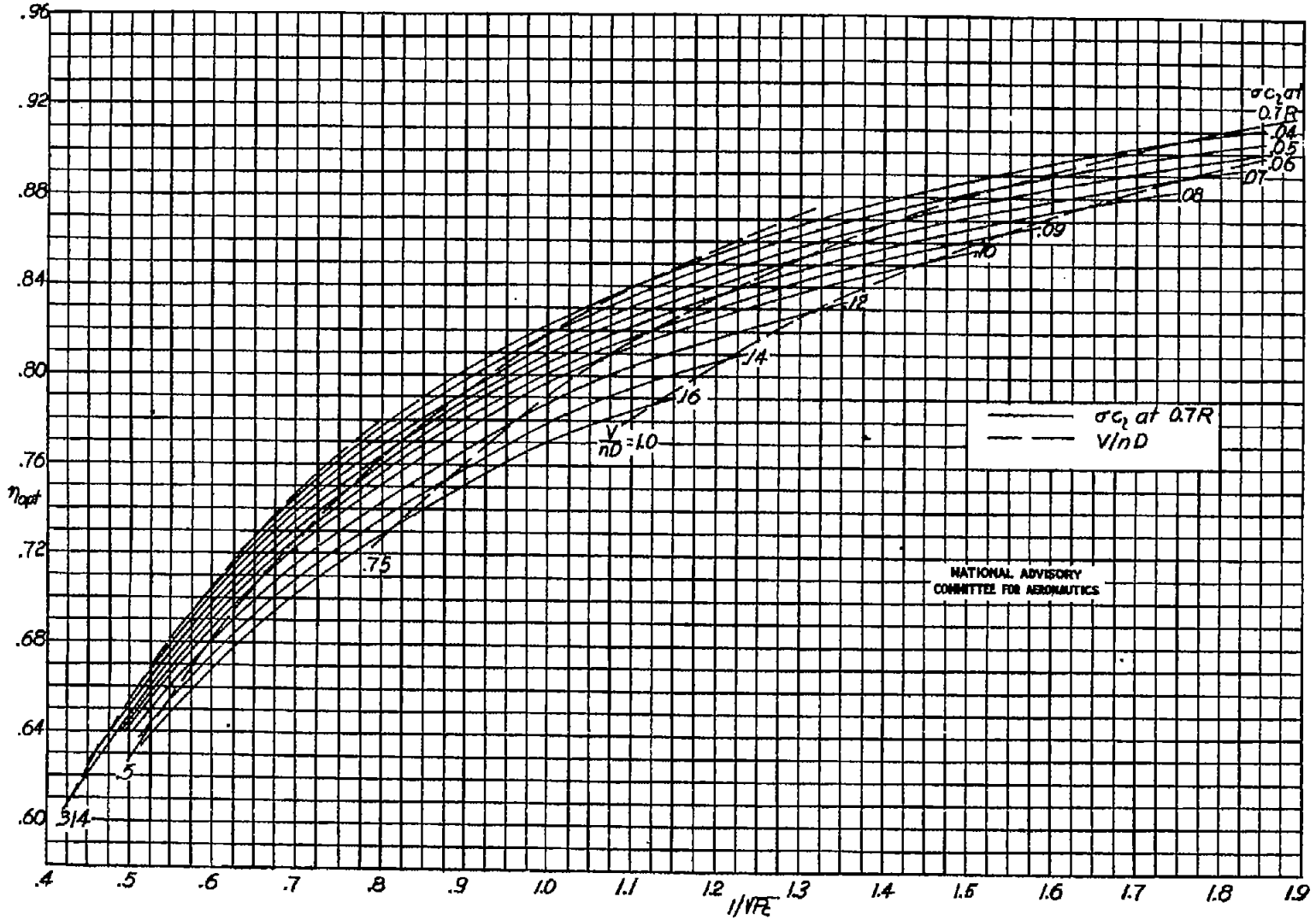

(b) Four-blade propellers.
Figure 25.- Continued.

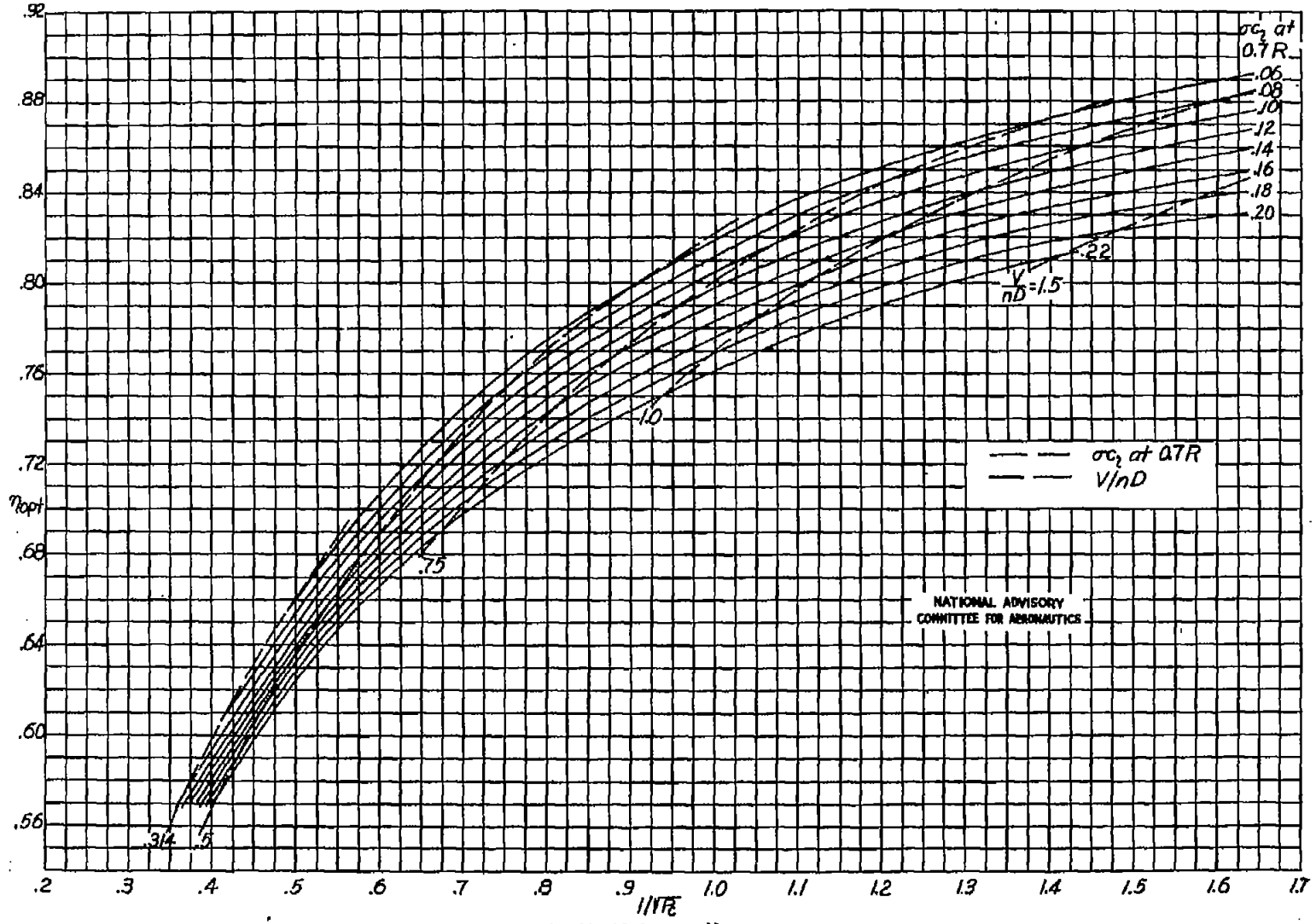

(c) Six-blade propellers.

Figure 25.- Continued.

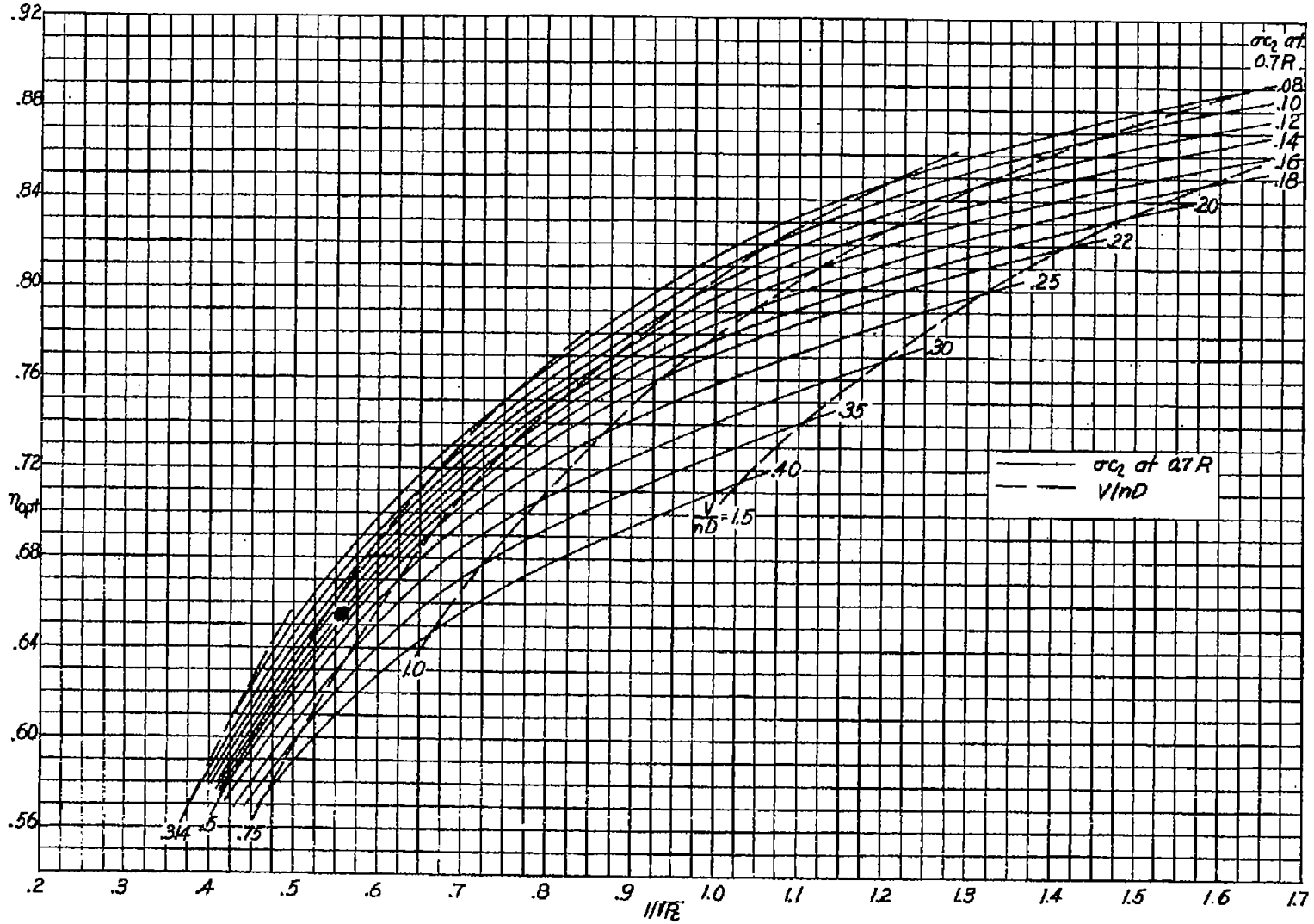

(d) Eight-blade propellers.

Figure 25.- Concluded.

NATIONAL ADVISORY
COMMITTEE FOR AERONAUTICS.

——— Calculated for $\left\{\begin{aligned}\left(\frac{dC_T}{dx}\right)_D &= -\sigma c_d \frac{\pi x}{4} \frac{J^2(1+a)^2}{\sin\varphi} \\ \left(\frac{dC_Q}{dx}\right)_D &= \sigma c_d \frac{\pi x^2}{8} \frac{J^2(1+a)^2}{\sin^2\varphi}\cos\varphi\end{aligned}\right\}$ where σc_l at 0.7R = 0.09

------ Calculated for $\left\{\begin{aligned}\left(\frac{dC_T}{dx}\right)_D &= -\sigma c_d \frac{\pi x}{4} J\sqrt{J^2+(\pi x)^2} \\ \left(\frac{dC_Q}{dx}\right)_D &= \sigma c_d \frac{\pi^2 x^3}{8} \sqrt{J^2+(\pi x)^2}\end{aligned}\right\}$

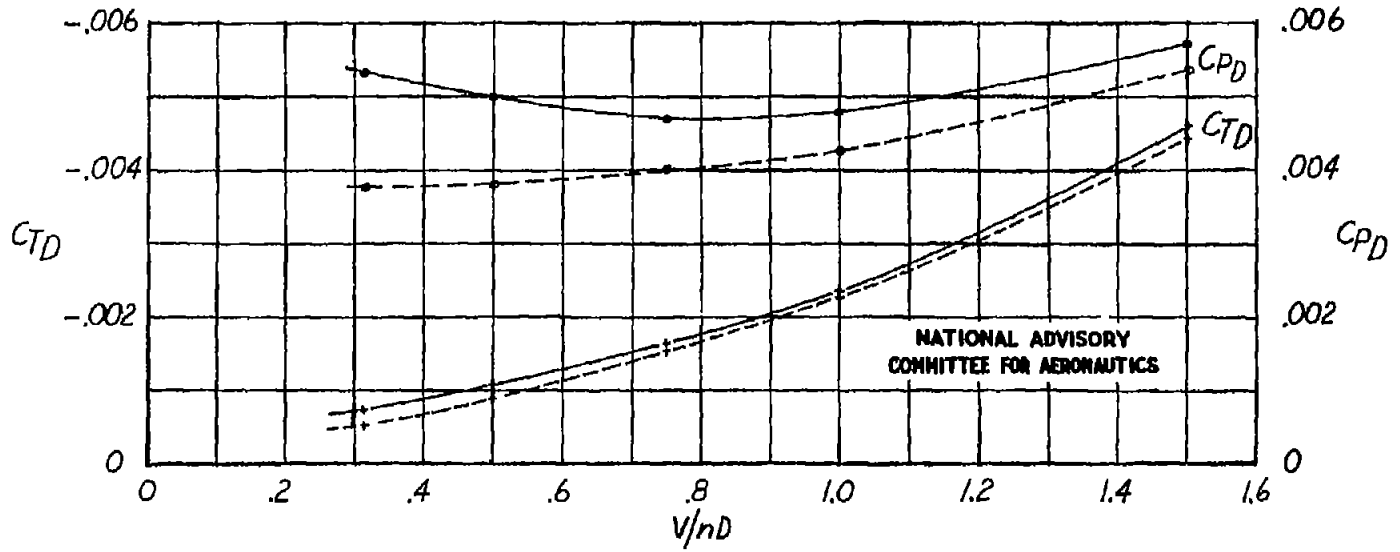

Figure 26.- Variation of thrust and power coefficients due to drag with V/nD for constant drag distribution. B = 4.